A Project Report on

DESIGN AND IMPLEMENTATION OF THREE PORT CONVERTER AND INVERTER FED BLDC MOTOR DRIVE FOR INDUSTRIAL APPLICATIONS

Submitted in partial fulfilment of the requirements for the award of the degree of

Bachelor of Technology

in

Electrical and Electronics Engineering

by

V. Tanmaya Tulasi (18FE1A0265) V. Rajarshi (18FE1A0268)

Y. Kishore Babu (18FE1A0271)

Under the esteemed guidance of

Dr. M.DIVYA.,Ph.D.,

Associate Professor

Department of Electrical and Electronics Engineering

VIGNAN'S LARA INSTITUTE OF TECHNOLOGY & SCIENCE

(An ISO 9001-2015 Certified, Approved by AICTE, New Delhi)

(**Affiliated to Jawaharlal Nehru Technological University Kakinada, Kakinada)**

Vadlamudi – 522213, Guntur District, Andhra Pradesh,

2021-2022

VIGNAN'S LARA INSTITUTE OF TECHNOLOGY & SCIENCE

(Affiliated to Jawaharlal Nehru Technological University Kakinada, Kakinada)

Vadlamudi – 522 213, Guntur District, Andhra Pradesh

Department of Electrical and Electronics Engineering

CERTIFICATE

This is to certify that this dissertation entitled as **"DESIGN AND IMPLEMENTATION OF THREE PORT CONVERTER AND INVERTER FED BLDC MOTOR DRIVE FOR INDUSTRIAL APPLICATIONS"** is being submitted by 1) V. Tanmaya Tulasi (18FE1A0265), 2) Y. Kishore Babu (18FE1A0271), 3) V. Rajarshi (18FE1A0268) of IV B.Tech., II semester, Electrical and Electronics Engineering branch, is a record of bonafide work carried out by them, in partial fulfillment of the requirements for the award of the **Degree in Bachelor of Technology** in **Electrical and Electronics Engineering.**

Project Guide	**Head of the Department**
Dr. M.DIVYA	**Dr. M.VENKATESAN**
Associate Professor	Professor

DECLARATION

We, the students of Vignan‘s Lara Institute of Technology & Science, Vadlamudi, Guntur District, Andhra Pradesh, here by declare that this Project Work titled as– “**DESIGN AND IMPLEMENTATION OF THREE PORT CONVERTER AND INVERTER FED BLDC MOTOR DRIVE FOR INDUSTRIAL APPLICATIONS”**, being submitted to the Department of Electrical and Electronics Engineering of this Institute, affiliated to Jawaharlal Nehru Technological University Kakinada, Kakinada, for the award of the Degree in Bachelor of Technology in Electrical and Electronics Engineering is a record of bonafide work done by us at ‘**VIGNAN’S LARA INSTITUTE OF TECHNOLOGY & SCIENCE**’ and it has not been submitted to any other Institution / University for the award of any other Degree.

Sl.No	Name	Roll. No	Signature
1	V.TANMAYA TULASI	18FE1A0265	
2	Y. KISHORE BABU	18FE1A0271	
3	V. RAJARSHI	18FE1A0268	

Place: Vadlamudi

Date:

ACKNOWLEDGEMENT

The satisfaction and the atrophic after the completion of any work would be incomplete without the mention of the people behind the successful completion of the work.

We acknowledge and express our sincere thanks and deep sense gratitude to the beloved chairman **Dr. LAVU RATHAIAH GARU** and the college management for providing us such a nice environment and good facilities for successful completion of the project.

We express our sincere thanks to **Dr. K.PHANEENDRA KUMAR**, Principal of Vignan's Lara Institute of Technology and Science, Vadlamudi, for providing us an excellent environment for doing this project.

We express our sincere thanks and Deep sense of gratitude to our Head of the Department **Dr. M.VENKATESAN,** for his patience and guidance that enabled to complete the project work.

We would like to express deep sense of gratitude to our guide **Dr**. **M.DIVYA** Associate Professor, Department Of Electrical And Electronics Engineering, Vignan's Lara Institute Technology of Science, Vadlamudi for his eminent guidance, cooperation in completion of this project work.

We are indebted to our faculty members, parents and friends for their co- operation and encouragement throughout the completion of this project.

CONTENTS

LIST OF FIGURES

LIST OF TABLES

NOMENCLATURE

S.NO	SYMBOL	NAME
1	I_L	Light-generated Current
2	I_d	Diode Current
3	I_{sh}	Shunt current
4	I_0	Diode reverse Saturation Current
5	V_T	Thermal voltage
6	n	Diode Ideality Factor
7	K	Boltzman Constant
8	R_S	Series resistance
9	R_{Sh}	Shunt resistance
10	I_M	Module Current
11	V_M	Module Voltage
12	$R_{DS\text{-}on}$	Drain-source Resistance
13	K_P	Proportional Gain
14	K_I	Integral Controller Constant
15	K_d	Derivate Control Constant
16	V_{bat}	Battery Voltage
17	P_{bat}	Battery power
18	m	Modulation Index
19	T_e	Electromagnetic Torque

LIST OF ABBREVIATIONS

ABBREVIATIONS	EXPANSION
PV	Photo Voltaic
MPPT	Maximum Power Point Tracking
DC	Direct Current
AC	Alternate Current
R	Resistance
L	Inductance
C	Capacitance
H	Solar Energy
I-V	Current–Voltage
V-P	Voltage-Power
P&O	Perturbation & Observation
ITPC	Integrated Three Port Converter
BLDC	Brush Less Direct Current
Z	Impedance
MATLAB	Matrix Laboratory
MOSFET	Metal Oxide Semiconductor Field Effect Transistor
BCD	Battery Charging Domain
PVD	PV space

BDD	Battery Discharging Domain
WEC	Wind Energy Conversion System
SC	Solar Cells
PID	Proportional-Integral-Derivate Controller
PI	Proportional and integral controllers
PD	Proportional and derivative controllers
FLC	Fuzzy Logic Controller
BMS	Battery Management System
SOC	State of Charge
Ni MH	Nickel Metal Hydride
Ni-cd	Nickel Cadmium
OCV	Open Circuit Voltage
LCB	Bidirectional Converter Local Controller
VSI	Voltage Source Inverter
CSI	Current Source Inverter
VFI	Voltage Fed Inverter
PWM	Pulse Width Modulation
KCL	Kirchhoff Voltage Law
KVL	Kirchhoff Current Law
PMSM	Permanent Magnet Synchronous Motor
SOC	State of Charge

ABSTRACT

With the proliferation of renewables and energy storage, inverters and converters are being updated to outperform their antecedents in every possible aspect for numerous applications in fields and industries. This project involves the design and implementation of improved three interface converter, and B4-Inverter fed brushless direct electric current motor drive for industrial uses. The proposed integrated Three Port Converter (ITPC) and B4-Inverter fed Brushless Direct Current Motor (BLDC) drive is proposed targeting low or medium applications. The ITPC has been operated in unidirectional and going in both directions for accomplishing a built-in dual electric potential and power rate of flow control. It also involves design of MPPT controller to extract maximum power from the converter under various operating conditions. The static and dynamic response of the converter has been controlled with various controllers like PID controller and fuzzy controller and the comparison has been provided among various controllers. The results are validated by performing simulations of the proposed systems in MATLAB/Simulink

CHAPTER 1
INTRODUCTION

1.1 Introduction

The constant development in demand for global energy along with the soaring awareness of the society about environmental effects due to the extended usage of fossil fuels has resulted in renewable energy sources, such as photovoltaic (PV) technology, to be popularly explored. Even though PV energy has gained significant attraction over the past few years, the discontinuous nature of PV systems and the low conversion efficiency concerning PV modules are the huge obstructions for exploiting the PV source on a massive scale. Hence, various studies have been carried out to minimize such disadvantages. For the purpose of extracting the maximum power of the PV array, the conventional implementation of the maximum power point tracking (MPPT) in stand-alone systems is usually achieved by serially connecting a DC-DC converter between the PV array and the load and then having a bidirectional DC-DC converter in a parallel connection between the energy storage element and the load. Energy storage element, such as the battery, is necessary for improving the system dynamics and steady-state characteristics. An Integrated Three Port Converter (ITPC) interfaced with solar, battery and motor, at the same time, can be considered to be a right candidate for a renewable power system and has gained a lot of research interest recently. Conventionally, one PV energy converter is needed for the maximum power point tracking and then, the entire power is stored in a series-connected battery. Then one battery discharging converter is required for load voltage control in a standalone system—nonetheless, the system bulk and the cost of battery rise owing to this series setup. Meanwhile, the efficiency of the system reduces

because of the two-stage conversion. The two-stage converter requires complicated PWM controls as a more significant number of capacitors and diodes are required for controlling the output voltage and state (charge/discharge level) of the battery. As an alternative to reduce conversion stages, one PV energy converter, one battery charging converter, and one battery discharging converter is proposed for standalone PV-battery system. However, there is an increase in the system losses because of this sophisticated architecture. Modified multilevel cascaded H-bridge inverters have also been studied for use in PV Systems. Consecutively, to decrease the control losses, additional ITPC architecture is introduced. ITPC features include one stage conversion connecting two of the three ports, greater system efficiency, and a smaller quantity of components, quicker response, and integrated power management among the ports with central control. The ITPC design. The current study explains the ITPC used B4-inverter fed BLDC motor drive system, having all the aforementioned benefits. In addition, it is possible to increase the total efficiency of the system in comparison with the existing one. The choice of BLDC motors for this paper emerged from their relative advantages over induction motors. The B4- inverter is an alternative topology of the conventional B6 inverter, having six switches and six diodes. B4-inverter fed BLDC motor drives have garnered a lot of attention in several works. Researchers have worked on renewable energy fed BLDC drive with a DC-DC converter for reducing vibration and noise. Several control schemes are prevalent for BLDC motor drives, such as FPGA based scheme sensor-less control etc. Compared with the traditional inverter, the Z-source inverter has an extra shoot through switching state. During the shoot- through state, the output voltage to the load terminals is zero, i.e., both the thyristors of the same leg conduct simultaneously. This period helps in boosting the voltage of the Z-impedance network. This shoot-through period is forbidden in conventional inverters which destroy the inverter.

1.2 Literature Survey

Sathish Kumar Shanmugam [1] et al., proposed design and implementation of improved three interface converter, and B4-Inverter fed brushless direct electric current motor drive for industrial uses. The proposed integrated Three Port Converter (ITPC) and B4-Inverter fed Brushless Direct Current Motor (BLDC) drive is proposed targeting low or medium applications. The ITPC has been operated in unidirectional and going in both directions for accomplishing a built-in dual electric potential and power rate of flow control. besides, efficiency and the losses of the proposed converter are analyzed using three different domains, i.e., battery charging, discharging, and photovoltaic (PV) effectively. The results are validated by performing simulations of the proposed systems in MATLAB/Simulink. The validation results reveal that the proposed converter works under all three domains and that the losses in the PV domain are reduced compared to the other converters. Also, the average efficiency achieved is 80.95%. These results authenticate the application of the proposed converter to numerous applications pertaining to renewable energy resources and energy systems.

Sathish Kumar Shanmugam [2] et al., proposed an implementation of solar photovoltaic array and battery powered enhanced dc-dc converter using B4-inverter fed brushless dc motor drive system for agricultural water pumping applications. It consists of step up and step-down converter, DC-link module. DC-link switching is achieved by reduced ripple voltage which results in improved quality of obtained output power. The Three Port Converter has been proposed and operated in unidirectional and/or bidirectional way simultaneously, for achieving an inherent dual voltage and power flow control. Switch count makes the system more cost effective. An excellent tracking performance under dynamic condition with negligible

oscillations around optimum operating point is achieved. Optimally selecting the initial value of duty ratio and its perturbation size offer soft starting of BLDC motor by slowly increasing the DC-link voltage of VSI. A simulation model of solar photovoltaic array and battery powered enhanced DC-DC converter is developed and its performance is analysed for various operating conditions.

Deng [3] et al., a novel three-port dc/dc topology is proposed for this application. Pulse width and phase shift offer two degrees of freedom to effectively regulate the power flows. On the primary side, the input current ripple is reduced due to the interleaved structure. This avoids the usage of the bulky electrolytic capacitor on the PV terminal. On the secondary side, a voltage six folder rectifier is employed to boost the step-up ratio. This reduces the turns number on the secondary-side of the transformer. Moreover, the voltage stresses of secondary-side MOSFETs and diodes are reduced to one-third of the output voltage. Zero-voltage switching and zero-current switching are realized among all power MOSFETs and diodes respectively and in an extended range. A 500 W converter prototype, linking a 40 V-60 V battery pack, a 20 V-30 V PV panel, and a 760 V dc bus, is designed and tested to verify the proof-of-concept. Both the circuit functionality and theoretical analysis are validated by the experimental results.

Objectives

- This project involves design of three port DC-DC converter with solar input.
- It involves design of various controllers based MPPT fed converter to control the output from the solar energy.
- It involves design of inverter for the operation of BLDC motor attaining input from converter.
- It also involves design of battery with bidirectional converter for steeping up or stepping down the voltage based on input condition.

CHAPTER 2
PROPOSED CONTROLLERS BASED MPPT FED SOLAR CONVERTER

2.1 Solar Energy

Solar energy is radiant light and heat from the sun that is using a rage of ever evolving technologies such as solar heating, photovoltaic, solar thermal energy, molten salt power plants and artificial photosynthesis.

It is an essential source of renewable energy and its technologies are broadly characterized as either passive solar or active solar depending on how they capture and distribute solar energy or convert it into solar power. Active solar techniques include the use of photovoltaic systems, concentrated solar power and solar water heating to use the energy. Passive solar designed refers to the use of the sun's energy for the heating and cooling of living spaces by exposure to the sun. When sun light strikes a building, the building materials can reflect, transmit or absorb the solar radiation.

The United Nations development program in its 2000 world energy assessment found that the annual potential of solar energy was 1575-49835 exajoules (EJ). This is several times larger than the total world energy consumption, which was 559.8 EJ in 2012. By using this, we can reduce the pollution, lower the cost of mitigating global warming and keep fossil fuel prices lower than otherwise. Solar energy is one of the purest and clean forms of energy we receive on earth, without any environmental degradation. Thanks to the never-ending solar radiations we receive, it is responsible for all the life processes taking place on earth. If we tap into this energy systematically, this can be the largest source of energy, and even a tenth of energy

from solar rays on earth can solve the entire energy crisis In India, however, the potential of energy from solar rays is about 750GW. If this energy is utilized, we won't need any other source of energy in our country. There are many ways converting solar energy to electricity, but most widely used ones are by using photo-voltaic cells (also called solar cells) and concentrated solar power, where solar rays are focused and the concentrated power generates heat to run the solar plant. Solar energy has gained a lot of significance in recent decade, due to shortage of non-renewable sources of energy. As on 30 June 2015, the installed grid connected solar power capacity is 4,060.65 MW, and India expects to install an additional 10,000 MW by 2017 and a total of 100,000 MW by 2022. India being the first country in the world to setup the ministry of non-conventional energy resources, Gujarat has been a leader in solar power generation and contributes 2/3rd of the 900 MW of photovoltaic in the country There have been a few initiatives from the government, such as the Indian Solar Loan Programme, which has focused on financing solar home power systems, to increase the use of solar energy for domestic use. It may also include lighting, irrigation or water heaters. Notably, Bangalore city has the largest deployment of solar water heaters in India. Solar industry has Investment 2015 also highlights a record $119 billion in new investment. Gujarat and Rajasthan alone account to more than 88% of total solar energy produced in India. As an entrepreneur, the potential for innovation is endless in this sector, as the whole world is moving in a direction to minimize the use of renewable energy and opting for solar devices. Right from automobiles to domestic appliances and handheld devices, solar is going to dominate the market in our near future. Moreover, as the efficiency of solar cells is less than 10%, there is huge scope for innovators to develop energy efficient solar devices and make it cost-effective to address the demands of the large population in our country.

- **Solar Panel:**

Solar panels get energy from the sun, for consumers to use. There are two types of solar panels, one is that collects the heat and the another one is that produce the energy. Heat fromsolar panel is often used for space heating and for hot water.Solar panels have become much cheaper to use compared to oil, diesel and liquefied natural gas in parts of Asia. Solar energy will soon become the main source of energy. Solar panels can be used for wide variety of applications including remote power systems for cabins, telecommunications equipment, remote sensing, and of course for the production of electricity by residential and commercial solar electric systems.

Fig 2.1: Solar Panel

2.1.1 Photo Voltaic (PV) Cell:

A photovoltaic cell is a solid-state electrical device that converts the energy of light directly into electricity by the photovoltaic effect. The energy of light is transmitted by photons-small packets or quantum of light. Electrical energy is stored in electromagnetic fields, which in turn can make a current of electrons flow.

Assemblies of solar cells are used to make solar modules which are used to capture energy from sunlight. When multiple modules are assembled group of modules all oriented in one plane is referred as a solar panel.

Solar cells are described as being photovoltaic irrespective of whether the source is sunlight or an artificial light. They are used as a photo detector, detecting light or other electromagnetic radiation near the visible range or measuring light intensity.

2.1.2 Working of PV Cell:

Photovoltaic cells are made based on the principle of photovoltaic effect. When the light reaches the p-n junction the light photons can easily enter in the junction through very thin p-type layer. The light energy, in the form of photons, supplies sufficient energy to the junction to create a number of electron-hole pairs. The incident light breaks the thermal equilibrium condition of the junction. The free electrons in the depletion region can quickly come to the n-type side of the junction. Similarly, the holes in the depletion can quickly come to the p-type side of the junction. Once, the newly created free electrons come to the n-type side, cannot further cross the junction because of barrier potential of the junction.

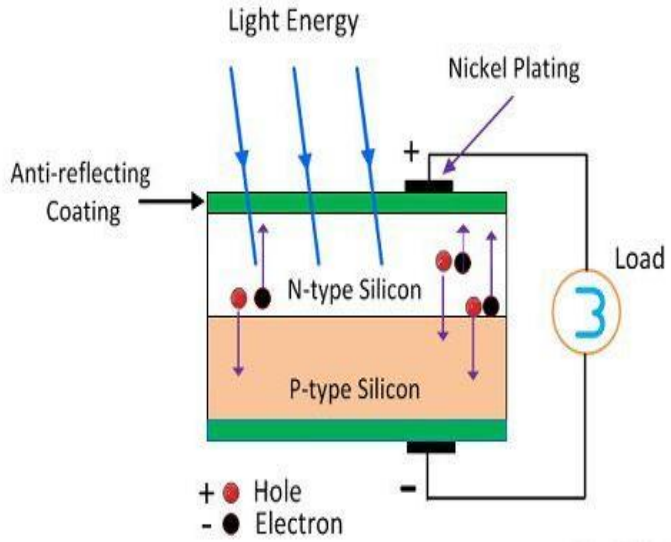

Fig 2.2 Working of PV cell

Similarly, the newly created holes once come to the p-type side cannot further cross the junction became of same barrier potential of the junction. As the concentration of electrons becomes higher in one side i.e., the n-type side of the junction and the concentration of holes become more in another side, i.e., the p-type side of the junction, the p-n junction will behave like a small battery cell. A voltage is set up which is known as photo voltage. If we connect a small load across the junction, there will be a tiny current flow through it.

2.1.3 PV Cell Modeling:

Equivalent circuit models define the entire I-V curve of a cell, module, or array as a continuous function for a given set of operating conditions. One basic equivalent circuit model in

common use is the single diode model, which is derived from physical principles and represented by the following circuit for a single solar cell as shown in Fig2.5

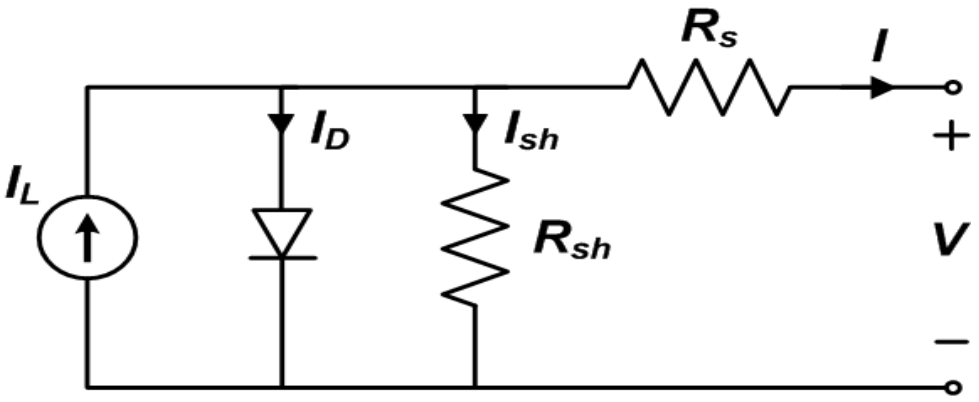

Fig 2.3: Single Diode PV Cell

The governing equation for this equivalent circuit is formulated using Kirchhoff's current law for current I.

$I = I_L - I_D - I_{sh}$ ..... (2.1)

Here, "I_L" represents the light-generated current in the cell

"I_D" represents the voltage-dependent current lost to recombination,

"I_{sh}" represents the current lost due to shunt resistances.

"I_D'' is modeled using the Shockley equation for an ideal diode.

$$I_D = I_0 \left[\exp\left(\frac{V+IR_s}{nV_T}\right) - 1\right] \ldots\ldots\ldots\ldots \text{(2.2)}$$

Where, n is the diode ideality factor.

I_0 is the saturation current,

and V_T is the thermal voltage given by

$$V_T = \frac{kT_C}{q} \ldots\ldots\ldots \text{(2.3)}$$

Where 'k' is Boltzmann's constant & 'q' is the elementary charge.

shunt current (I_{sh}) as follows

$$I_{sh} = (V + IR_s)/R_{sh} \ldots\ldots\ldots \text{(2.4)}$$

The complete governing equation for the single diode model is as follows

$$I = I_L - I_0 \left[\exp\left(\frac{V+IR_s}{nV_T}\right) - 1\right] - \frac{V+IR_s}{R_{sh}} \ldots\ldots\ldots \text{(2.5)}$$

The five parameters in this equation are primary to all single diode equivalent circuit models:

- I_L : Light current (A)
- I_0 : diode reverse saturation current (A)
- R_s : series resistance (Ω)
- R_{sh}: Shunt resistance (Ω)
- n : diode ideality factor (unitless).0

For a photovoltaic module or array comprising N_s, cells in series, and assuming all

cells are identical and under uniform and equal irradiance and temperature

$$I_{module} = I_{cell} \text{ and } V_{module} = N_s \times V_{cell} \quad \ldots\ldots\ldots (2.6)$$

The single diode equation for a module or array becomes

$$I_M = I_L - I_0 \left[exp\left(\frac{V_M + I_M N_S R_S}{n N_S V_T}\right) - 1 \right] - \frac{V_M + I_M N_S R_S}{N_S R_{sh}} \ldots\ldots\ldots (2.7)$$

Where I_M and V_M are the current and voltage respectively of the module or array. Care should be taken while implementing the model parameters, as they are either applicable to a cell, module, or array Parameters for modules or arrays, are strictly used with the single diode equation for I, which is more commonly implemented form.

2.2 Proposed DC-DC Converter

To demonstrate the dynamic output qualities of the PV module under various daylight conditions, the framework proposed will work in different power stream modes such as battery charging area (BCD), PV space (PVD) and battery releasing space (BDD). In the Battery Charging Domain (BCD) mode, the PV charges the battery. The bidirectional converter works as a buck converter in the BCD. This happens if the PV power is extremely contrasted with the heap control and if the PV voltage is higher than the battery voltage required, indicating that the battery must be charged. In BCD, switches S1, S2, S3 are dynamic and switch S4 is in off condition. BCD has four modes, which are named as mode A, B, C, and D. In mode A, the switch, S2, is turned on and switches S1, S3, S4 are off. As S2 is on, energy stored in the inductor L1 moves to the capacitor C1, and the capacitor begins to charge. The identical circuit of ITPC working in this mode is demonstrated. In mode B, the switch S1 is turned on and switches S2, S3, S4 are off. Since S1 is on, the inductor L1 begins to charge from PV, and afterward, the current, iL1 increases. Then again, the current in the capacitor, iC1 and PV begin to release to the output capacitor, CO2 through the

diode, D2, and current, iC1 reduces, while the output capacitor current, IO2 increases. The proportional circuit of ITPC working in this mode demonstrated as the blue line in Figure 6. In mode C, the switch, S3 is turned on and switches S1, S2, S4 are turned off. Also, the extra energy in the inductor, L1, moves to the battery, while the battery starts to charge. All the while, the diode, D1is forward biased for making a flowing current way of the inductor, L1, subsequently the capacitor, CO1 current increases. The identical circuit of ITPC working in this mode is demonstrated as a green line in Fig 2.2: Working of PV Cell Figure 6. In mode D, switches, S2 and S3 are turned on and switches S1, S4 are turned off. The extra energy present in the inductor, L1 gets moved to the battery while the battery starts to charge. Simultaneously, the inductor, L1, begins to release energy to the capacitor, C1 through a switch, S2, and the capacitor current, iC1 increases. The comparable circuit of ITPC working in this mode is signified as a green and red line in Figure 6 correspondingly. In the PVD mode, the value of the load current is equal to the PV module current; the power that is handled by the bidirectional converter is zero. Here, the efficiency of the power network is near 95% since the most extreme intensity of the PV module gets moved to the load just by the DOBB converter. In PVD, switches S1 and S2 are dynamic and switches S3 and S4 are completely off. In the BDD mode, both the sources PV and battery provide energy to the load. The bidirectional converter works as a boost converter either in the battery de-energize mode or if the load power demand is higher than the produced power. In BDD, switch, S3 is turned off entirely, and switch S1, S2, S4 are dynamic. The five various activity modes in BDD are modes H, I, J, K and L. In mode H, the switch, S2 is turned on and switches S1, S3, S4 are turned off. Since S2 is on, the energy stored in the inductor L1 flows to the capacitor C1, and the capacitor begins to charge. The proportional circuit of ITPC working in this mode is shown as a red line in Figure 7. In mode I, the switch S1 is turned on and switches

S2, S3, S4 are turned off. As S1 is on, the inductor, L1 begins to charge from PV, and the current, iL1 increases. Then again, the current in the capacitor C1 and PV begins to release to output capacitor, CO2 through the diode D2, while the output capacitor current increases. The equal circuit of ITPC working in this mode is meant as the blue line in Figure 7. In mode J, the switches S1 and S4 are turned on and switches S2 and S3 are turned off. In this way, the inductor, L1 begins to charge from PV, while the current in the capacitor, C1 and PV begin to release to output capacitor, CO2 through the diode, D2. At the same time, the surplus load current gets removed from the battery and afterward put away in an inductor, L1 through a switch, S4 and diode, D3. The comparable circuit of ITPC working in this mode is demonstrated as a green line in Figure 7. In mode K, switch S4 is turned on and switches S1, S2 and S3 are turned off. In this way, the surplus load current is removed from the battery and afterward, put away in an inductor, L1, consequently, the inductor current increases. The identical circuit of ITPC working in this mode is shown as a green line in Figure 7. In mode, L switches S1, S2, S3, and S4 are turned off. In this way, the surplus current put away in an inductor, L1 gets moved to the output capacitor, CO1.

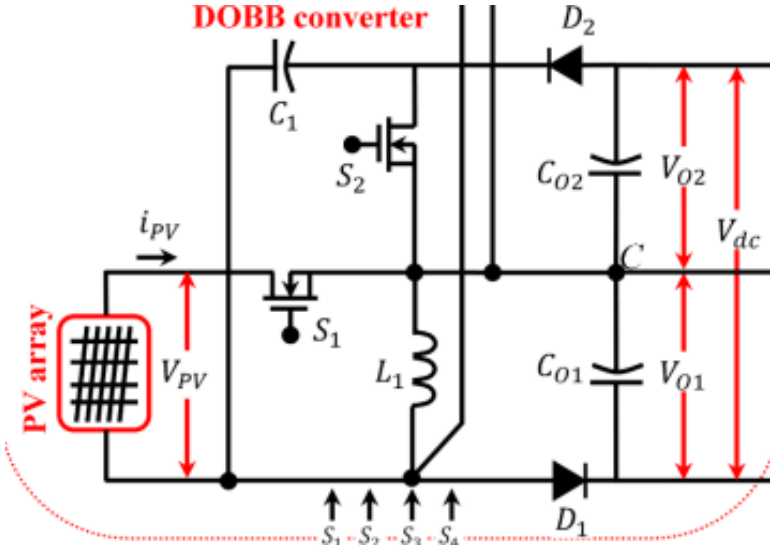

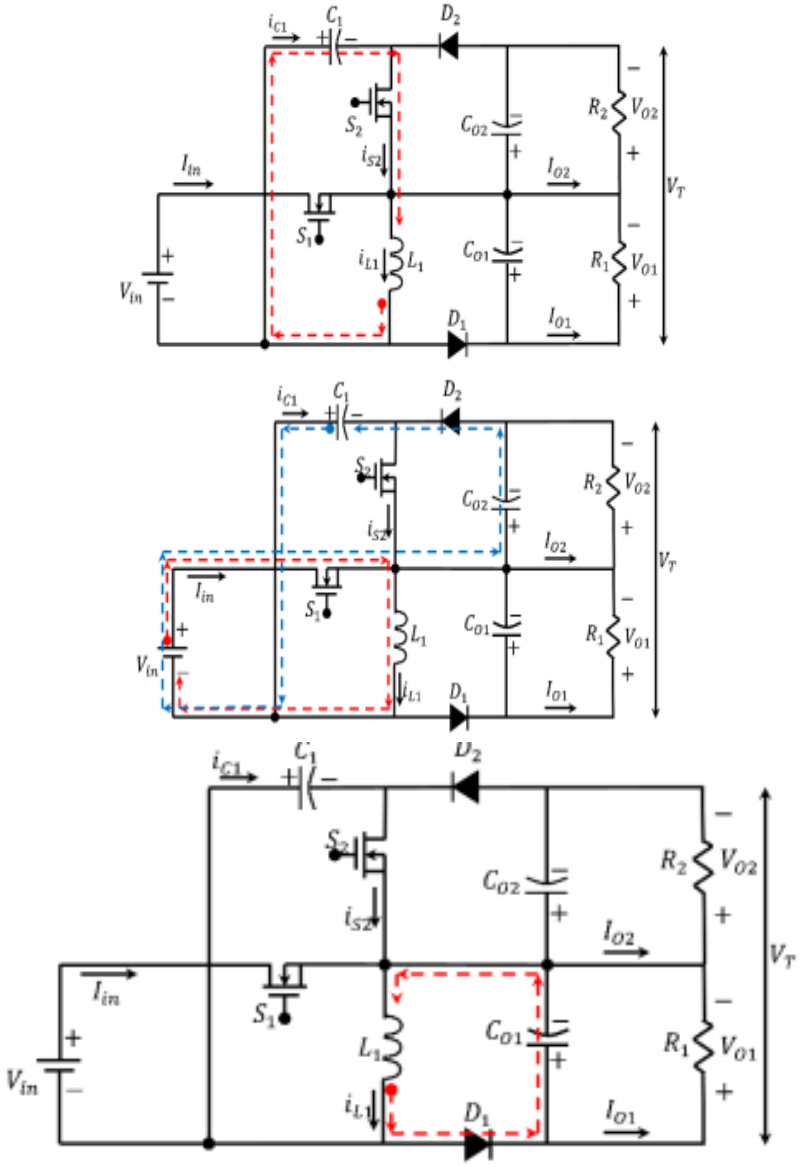

Fig 2.4: ITPC Conducting states at a time interval (a) 1; (b) 2; (c) 3,showing the flow of current in different modes of operation marked in red and blue.

The converter conduction at different time intervals and its modelling are shown in Figure (a). During the conduction at time interval 1 as represented, the governing equations are

$$L_1 \frac{di_{L1}}{dt} = -V_{C1}$$

$$C_{01} \frac{dV_{01}}{dt} = -\frac{V_{01}}{R_1}$$

$$C_{02} \frac{dV_{02}}{dt} = -\frac{V_{02}}{R_2}$$

During the conduction at time interval 2 as represented in Figure (b), the governing equations are

$$L_1 \frac{di_{L1}}{dt} = V_{in}$$

$$C_{01} \frac{dV_{01}}{dt} = -\frac{V_{01}}{R_1}$$

$$C_{02} \frac{dV_{02}}{dt} = \frac{V_{C1}+V_{in}-V_{02}}{R_2}$$

During the conduction at time interval 3 as represented in Figure (c), the governing equations are

$$L_1 \frac{di_{L1}}{dt} = -V_{01}$$

$$C_{01} \frac{dV_{01}}{dt} = i_{L1} - \frac{V_{01}}{R_1}$$

$$C_{02} \frac{dV_{02}}{dt} = -\frac{V_{02}}{R_2}$$

Conduction loss of the switch S1 is

$P_{cond-S1} = I_{S1}^2 \times R_{DS-on}$

where, I_{S1} denotes the current flowing through the switch S1, and $R_{DS\text{-}on}$ represents the drain to source resistance of the switch when it is in a conducting state or on the state.

2.3 MPPT With Various Controllers

A controller is a mechanism that seeks to minimize the difference between the actual value of a system and the desired value of the system. Controllers are a fundamental part of control engineering and used in all complex control systems. Before we introduce you to various controllers in detail, it is very essential to know the uses of controllers in the theory of control systems. The important uses of the controllers include.

- Controllers improve the steady state accuracy by decreasing the steady state error.
- As the steady-state accuracy improves, the stability also improves.
- Controllers also help in reducing the unwanted offsets produced by the system.
- Controllers can control the maximum overshoot of the system.
- Controllers can help in reducing the noise signals produced by the system.

MPPT CONTROLLER:

Recently, renewable energies, in general, and solar energy, in particular, have received intensive research interests, due to their abundant and environmentally friendly characteristics. In solar energy systems, photovoltaic (PV) systems are used to directly convert light into electricity. Due to its volatility, solar energy in these systems should be converted as much as possible when it is available, and this can be done by applying maximum power point tracking algorithms. These algorithms are used to control the DC/DC converters, found in photovoltaic systems, to dynamically adapt its operating point to the maximum power point of the PV. There are many algorithms for finding the maximum power point (MPP) of solar panels. Some methods are simple and easy to control such as: Fractional Open-Circuit Voltage,

Fractional Short-Circuit Current, Perturb-and-Observe (P&O) and the Incremental Conductance (Inc Cond). However, there are complex methods for doing the task of tracking MPP such as Current Sweep, Fuzzy Logic Control and Artificial Neural Network. These complex methods require a lot of calculations and memory, implying the need to use more powerful microcontrollers due to heavier computational load than that of simple methods. Hence, this paper proposes a simpler method of maximum power point tracking (MPPT) with high accuracy.

Maximum power point tracking (MPPT) or sometimes just power point tracking (PPT), is a technique used commonly with wind turbines and photovoltaic (PV) solar systems to maximize power extraction under all condition.

Classification of MPPT techniques,

1. Perturb and observe.
2. Incremental conductance.
3. Constant voltage.
4. Temperature method.

These controller techniques are following the several strategies to optimize the power output of an array. Maximum power point trackers may implement different algorithms and switch between them based on the operating conditions of the array.

- **Perturb And Observe Algorithm**

The photovoltaic power systems are one of the fastest growing renewable energy technologies, providing more secure power sources and pollution free electric supplies. Unfortunately, PV systems have two major drawbacks: low efficiency of energy conversion and its nonlinear characteristics, which depend on the irradiation and temperature conditions. Therefore, to extract maximum power from the PV module, it is necessary to determine its operating point that provides the maximum power output from the photovoltaic panels. An MPPT system is used to extract the

maximum power from the PV module using boost converter as an interface between the PV module and load to transfer the maximum power of the photovoltaic system to the load. Maximum power is transferred by changing the load impedance as seen by the source and matching it at the peak power of it when the duty cycle is varied. In order to maintain PV module's operating at its MPP, different MPPT methods are studied. However, one algorithm, the perturb and observe claimed by many methods and continue to be by far the most common MPPT method used in practice because it is simple structure.

Perturb and observe algorithm is simple and does not require previous knowledge of the PV generator characteristics or the measurement of solar intensity and cell temperature and is easy to implement with analogue and digital circuits. It perturbs the operating point of the system causing the PV array terminal voltage to fluctuate around the MPP voltage even if the solar irradiance and the cell temperature are constants.

In order to increase the efficiency and to maintain the operating point at an optimum maximum power point of the PV power generation system, Maximum Power Point Tracking (MPPT) is used to track the new modified maximum power point in its corresponding curve whenever there is a variation in the temperature or irradiation and to keep maintain thispoint at an optimum value a power conditioner or a DC–DC converter is added as an interface between the PV generator and the load. It extracts the maximum power from the source and transfers it to the load by stepping up (boost) or stepping down (buck) as per the requirement at the load side. The power transfer is carried out in accordance to the maximum power value by varying the on/off duty cycle of switch of the DC-DC converter. The P&O method is widely used in MPPT, because it has a fewer measured parameter. It can track maximum power point quite accurately through variations in radiation and temperature. It operates by

perturbing the system by increasing or decreasing the panel operating voltage and observing the impact of this change on the panel output power. Moreover, it is the most widely used and workhorse MPPT algorithm because of its balance between performance and simplicity. However, it suffers from the lack of speed and C. It is simple and straightforward technique. The P&O method is frequently used for its simplicity. However, this method makes the operating power point fluctuate around the MPP and then leads to power loss. In the modified P&O, we add a stop condition for preventing the oscillation. When the absolute value of power variation ΔP is less

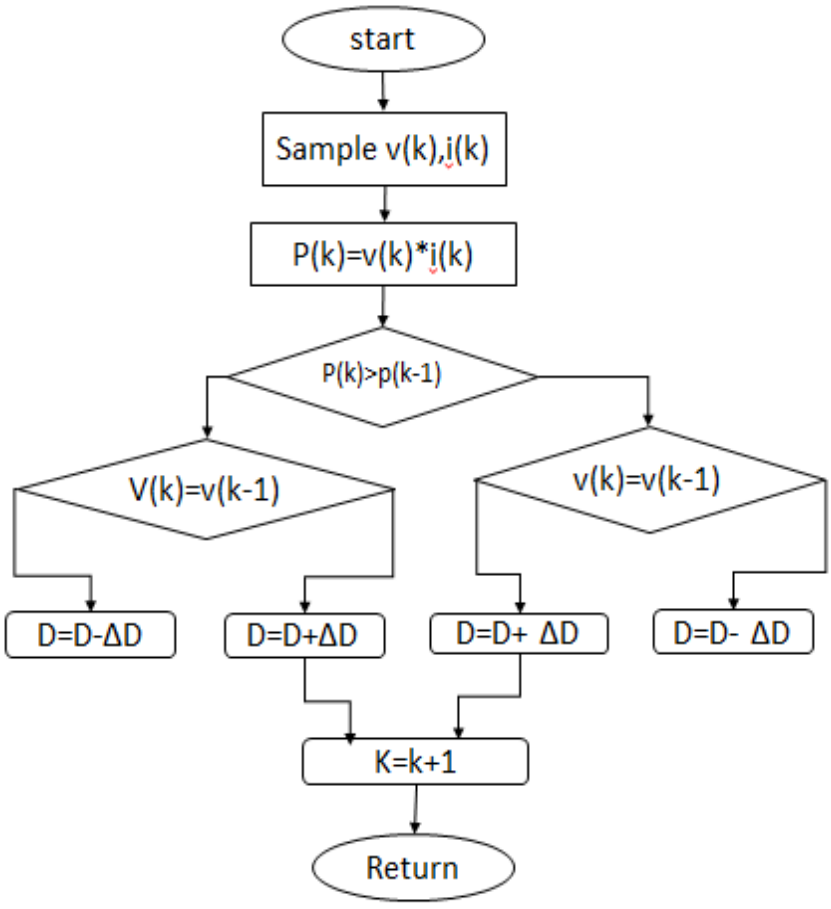

Fig 2.5: Flow Chart of Perturb and Observe Method

than an amount of εPO, the power point is near the MPP and we should not change the panel voltage until any detectable changes of temperature and/or irradiation. The flowchart of the modified P&O method. The duty cycle D of the DC/DC converter is initially set at D0. To control the panel voltage, we just need to add or subtract an amount of ΔD0 to the duty cycle. In the case that ΔD and ΔV equal to zero, the value of ΔP/ΔV is incalculable so that we have to consider the two cases of ΔP and ΔP/ΔV. The values of ΔP and ΔP/ΔV (ΔV is the voltage variation) are negative when the operating point is on the right side of MPP and vice versa. Therefore, we can use the sign of ΔP and ΔP/ΔV to determine the required change of the panel voltage for better power extraction from the PV.

In PV &WEC system applications, it is very important to design a system for operating of the Solar Cells (SCs) & pitch angel control of the WEC system under best conditions and highest efficiency. Maximum Power Point (MPP) varies depending on the angel of sunlight on the surface of the panel and cell temperature. Hence, the operating point of the load, PV systems are designed to include more than the required number of modules. Similarly in case of WEC for varying wind conditions. Pitch control comes handy when speed increases more than the rated speed, it will change pitch angel in such a way that it will rotate & constant speed to generate maximum power. The solution to this problem is that switching power converters are used, that is called Maximum Power Point Tracker (MPPT). In these projects, the various aspects of these algorithms have been analyzed in detail. Moreover, a comparison was made in the conclusion.

2.4 Proportional Integral Controller:

Feedback control is a mechanism that uses information from measurements. In

feedback control system, the output is sensed. There the two main types of feedback control systems:

1.Positive feedback

2.Negative feedback

The positive feedback is used to increase the size of the input but in negative feedback, the feedback is used to decrease the size of the input. The negative systems are usually stable. A PID is widely used in feedback control of industrial processes on the market in 1939 and has remained the most widely used controller in process control until today.

Thus, the PID controller can be understood as a controller that takes the present, the past, and the future of the error into consideration. After digital implementation was introduced, a certain change of the structure of the control system was proposed and has been adopted in many applications. But the change does not influence the essential part of the analysis and design of PID controllers. A proportional-integral-derivative controller (PID Controller) is a method of the control loop feedback. The main feature of continuous controllers is that the controlled variable can have any value within the controller's output range. Now in the continuous controller theory, there are three basic modes on which the whole control action takes place.

1. Proportional Controllers.
2. Integral Controllers.
3. Derivative Controllers.

We use the combination of these modes to control our system such that the process variable is equal to the set point. These three types of controllers can be combined into new controllers.

1. Proportional and integral controllers (PI Controller)
2. Proportional and derivative controllers (PD Controller)

3. Proportional integral derivative control (PID Controller)

- **Role of a Proportional Controller (K_p):**

The role of a Proportional depends on the present error, Integral depends on the accumulation of past error and Derivative on the prediction of future error. The weighted sum of these three actions is used to adjust Proportional control is a simple and widely used method of control for many kinds of systems. In a proportional controller, steady state error tends to depend inversely upon the proportional gain. The proportional response can be adjusted by multiplying the error by a constant Kp, called the proportional gain. The proportional term is given by

P=Kp*error (t)

A high proportional gain results in a large change in the output for a given change in the error. If the proportional gain is very high, the system can become unstable. In contrast, a small gain results in a small output response to a large input error. If the proportional gain is very low, the control action may be too small when responding to system disturbances. Consequently, a proportional controller (Kp) will have the effect of reducing the rise time and will reduce, but never eliminate, the steady-state error.

- **Role of Integral Controller (K_i)**

An Integral Controller (IC) is proportional to both the magnitude of the error and the duration of the error. The integral is in a PID controller is the sum of the instantaneous error over time and gives the accumulated offset that should have been corrected previously. Consequently, an integral control (K_i) will have the effect of eliminating the steady-state-error, but it may make the transient response worse.

- **Role of Derivative Controller (K_d)**

  The derivative of the process error is calculated by determining the slope of the error over time and multiplying this rate of change by the derivative gain Kd. The derivative term shows the rate of change of the controller output. A derivative control (Kd) will have the effect of increasing the stability of the system, reducing the overshoot, and improving the transient response**.**

  $$D= Kd(d(t))/dt)$$

- **Performance Analysis of K_p, K_i, K_d**

  The error signal e(t)is used to generate the proportional, integral, and derivative actions, with the resulting signals weighted and summed to form the control signal u(t) applied to the plant model.

Table-2.1 Tabular Form of PID Parameters

Parameter	**Rise Time**	**Overshoot**	**Settling Time**	**Steady-State Error**
k_p	Decrease	Increase	Small Change	Decrease
k_i	Decrease	Increase	Increase	Decrease Significantly
k_d	Minor Decrease	Minor Increase	Minor Decrease	No effect in theory

Where u(t) is the input signal to the multivariable processes, the error signal e(t) is defined as e(t)=r(t)-y(t), and r(t) is the reference input signal. A standard PID controller structure is also known as the "three-term'' controller. This principle mode of action of the PID controller can be explained by the parallel connection of the P,I and D elements of the block diagram of PID controller.

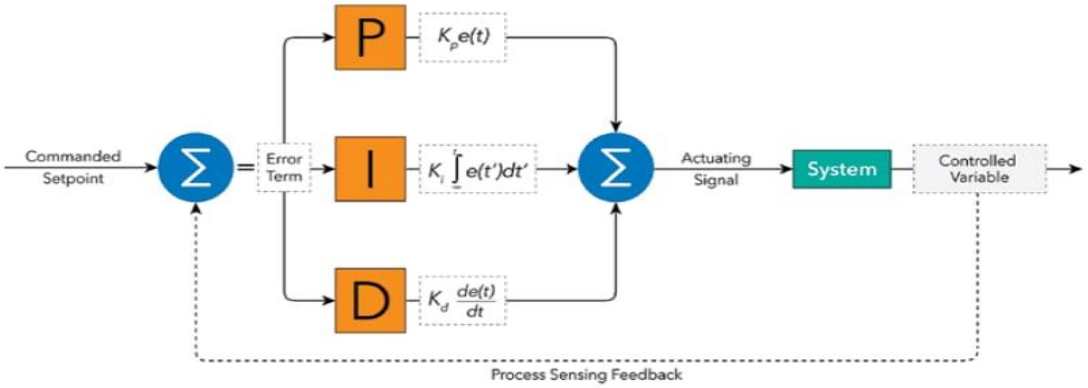

Fig 2.6: General structure of PID controller

The three variables P, I, D, are usually tuned within given ranges. Therefore, they are often called the tuning parameters of the controllers. By proper choice of these tuning parameters a controller can be adapted for a specific plant to obtain a good behaviour of the controlled system. In this project, multiple input and single output boost converter is used where the energy from PV cells and wind system can be taken as a input to the boost converter.

Classical dependent PID Equation:

$$u(t) = K_c e(t) + \frac{K_c}{\tau_i}\int_0^t e(t)dt + K_c\tau_d\frac{de(t)}{dt} \quad \text{..... (2.8)}$$

Classical independent PID Equation:

$$u(t) = K_c e(t) + K_i\int_0^t e(t)dt + K_c\tau_d\frac{de(t)}{dt} \quad \text{..... (2.9)}$$

Using the response for a step input, the step response r(t) of the PID controller can be easily determined

The main objective of DC-DC Boost converter is to maintain a constant output voltage despite variations in input/output source voltage, components and load current. Designers, aim to achieve better conversion efficiency, minimized harmonic distortion and improved power factor while keeping size and cost of converter within acceptable range. A simple PID controller has been applied to a conventional boost converter and tested in MATLAB Simulink environment achieving improved voltage regulation. The proposed closed loop implementation of the converter maintains constant output voltage despite changes in input voltage and significantly reduces overshoot thereby improving the efficiency of the converter.

2.5 Fuzzy Logic Controller:

The concept of fuzzy logic was introduced by Lotfi Zadeh (1965). A Fuzzy control system is a control system based on fuzzy logic, a mathematical system that analyses analog input values in terms of logical variables that take on continuous values between 0 and 1, which operates on discrete values of either 1 or 0 (true or false). In general, the fuzzy logic provides an inference structure that enable appropriate human reasoning capabilities. Fuzzy logic systems are suitable for approximate reasoning. Fuzzy logic systems have faster and smoother response than conventional systems and control complexity is less.

Basic Components in Fuzzy Control:

The three main components of a Fuzzy Logic controller are

1.Fuzzification

2.Fuzzy Rule base &Interfacing Engine

3.Defuzzification

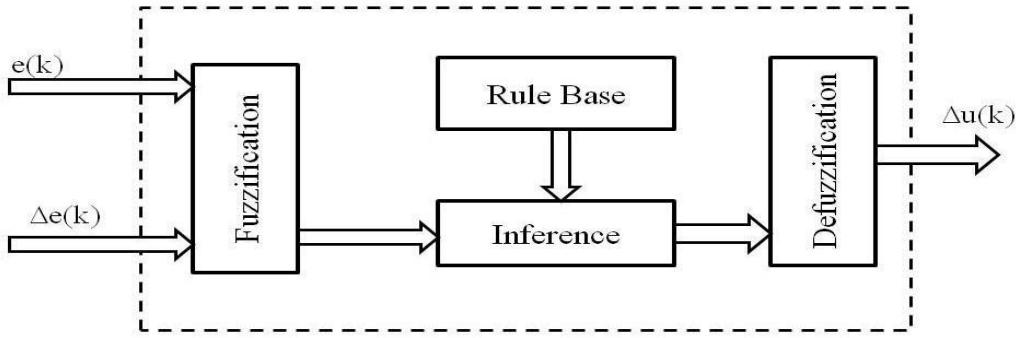

Fig 2.7: Fuzzy Control Internal Diagram

A. Fuzzification Module:

The most important step in formulating a design for the fuzzy controller is to identify the state variables which efficiently control the plant. After figuring out the state variables, they are to be passed through the fuzzification block to fuzzify the inputs as the FLC works with only the Fuzzy inputs. As the Fuzzy Rule base employs rules on only linguistic variables, the numerical inputs have to be converted to fuzzy linguistic variables first. This process of converting a numerical state variable into a fuzzy input linguistic variable is called Fuzzification process. The variables generally used comprise of state error, the rate of change of state error (derivative of state error), or the area of a state error (integral of state error). The membership function is the graphical representation of the degree of belonging of an element to the fuzzy set. We can use different membership functions for an input and output depending upon the requirement of the precision to be provided. Generally used membership functions are triangular and trapezoidal membership functions. Gaussian and Bell shaped are some other available membership functions. For number of membership functions, the accuracy of control increases and the control works effectively. Complexity and time delay due to calculations increase with the number of

membership functions taken for a linguistic variable. Hence, the number of membership functions to be used is a judgement that has to be made considering the quickness and efficiency of control to be delivered. In this model five membership functions for the Error and five membership functions for the Rate of change of error have been considered and the output has been given five membership functions.

B. Fuzzy Rule Inference:

Fuzzy inference is of two methods. They are

1. Mamdani.
2. Sugeno.

They are explained as below:

Mamdani Method:

Mamdani's methods of the Fuzzy interface is the most commonly used method. It was among the first control systems built using fuzzy set theory. It was first put forward by Ebrahim Mamdani as an attempt to control a steam engine and boiler combination by synthesizing a set of linguistic control rules obtained from experienced human operators. This inference method expects the output variable to be fuzzy sets. It is possible and also efficient to use a single spike in the output as membership function rather than a distributed fuzzy set. This is known as singleton output membership function. It enhances the Defuzzification process because it greatly simplifies the computation required by the more general Mamdani method which finds the centroid of the two-dimensional functions. But in the Sugeno type of inference can be used to model any inference system in which the output membership function is either linear or constant.

C. Defuzzification:

General methods adopted for Defuzzifying are:

1.Centre of Gravity Method,

2.Bisector of Area Method,

3.Mean of Minimum Method,

The converse of Fuzzification is called Defuzzification. The Fuzzy Logic Controller (FLC) produces output in a linguistic variable (fuzzy number). As indicated by true prerequisites, the linguistic variables must be changed to crisp output. Centre of gravity strategy is the best understood Defuzzification system and utilized as a part of this exploration work. It acquires the centre of gravity of a region involved in the fuzzy set. Defuzzification is the methodology of delivering a quantifiable result in the fuzzy form. A fuzzy control system has certain rules that change various variables into a "fuzzy" form, that is, the outcome is shown as membership functions and their degree of membership in fuzzy sets. The easiest but not much useful technique is to select the fuzzy set with the highest membership belonging, for this situation. The disadvantage of this methodology is that some data gets lost in this process. The rules that performed "Reduce Pressure" might as well have been absent with this process.

A helpful Defuzzification procedure should first include the outcomes of the results together somehow. The most average fuzzy set enrolment capacity has the shape of a triangle. Suppose, if this triangle were to be cut in a straight level line some place between the top and the base, and the top segment were to be removed, the remaining figure is in the shape of a trapezoid. This procedure removes parts of the figures to give trapezoids if the membership function used earlier was triangular (or different shapes if the initial shapes were not triangles). Generally, these trapezoids are superimposed one upon another, giving a single shape. Finally, the centroid of this is computed. The abscissa of the centroid gives the defuzzied output.

CHAPTER 3
BATTERY FED BIDIRECTIONAL CONVERTER WITH CHARGING AND DISCHARGING TOPOLOGY

3.1 Introduction

Batteries of PV systems are subjected to frequent charging and discharging process. Lead acid battery with deep discharge is commonly used for PV applications. Gel type lead acid batteries are used for remote applications where maintenance free operation is required. For portable applications Nickel-Cadmium or Ni-Metal hydride batteries are used. The life time of the batteries varies from 3 to 5 years. The life time depends on charging/discharging cycles, temperature and other parameters. The batteries for PV applications are to be designed to meet the following characteristics:

1. Low cost
2. High energy efficiency
3. Long life time
4. Low maintenance, robust construction
5. Good reliability and less self discharge
6. Wide operating temperature

Low Cost:

The cost can be represented by the initial cost or annual cost. The initial costs are the cost fixed during planning phase to purchase the storage batteries. The maintenance and operation costs need not be included in the initial cost. But these costs must be included in the annual cost calculation. The battery lifetime strongly influences the cost of the system. If the lifetime of the battery is less than 3.5 years then battery is the highest cost incurring component in the system.

Efficiency:

The battery units are not ideal. There may be energy losses during charging, discharging and self-discharging during unused time also. The energy efficiency is calculated as the ratio of charged energy to the discharged energy. Energy efficiency = charged energy (KW)/Discharged energy (KW). The self-discharge depends on internal leakage losses of the battery and external losses due to the energy consumption of electronic components. The self-discharge of the battery increases with increase in temperature. To reduce self discharge batteries should be stored at lower temperature.

Maintenance:

Low maintenance or maintenance free operation of battery is prepared for small systems at rural areas.

- Functions Of Storage Battery in a PV System

Energy storage and autonomy: To store electrical energy produced by the PV array and to supply energy to electrical loads as and when needed (during night time and non sunshine days in winter).

Stabilization of voltage: To supply power to electrical loads at stable voltages by suppressing voltage fluctuations in PV systems and protecting loads from damage.

Surge supply current: To supply the high starting currents to electrical loads such as motor or other inductive loads. The performance of the PV system with battery storage depends on the battery design and operating parameters of the system. If the battery is not designed for the operating conditions of the PV system then it will fail to work prematurely.

Micro grid systems, electric vehicles and portable devices need batteries as storage devices and power sources. A battery management system (BMS) is critical for maintaining optimum battery performance. A BMS consists of charging-discharging

strategies, state-of-charge (SOC), voltage balancing, and temperature measurement. It is important to design an appropriate battery management system (BMS) for maintain optimum battery storage performance. Today most common battery technologies are based on lead, sodium, nickel and lithium electro chemistries. A lithium-ion battery is a type rechargeable battery, where lithium ions move from the negative electrode to positive electrode during discharge &The process is reversed during charging. Li-ion

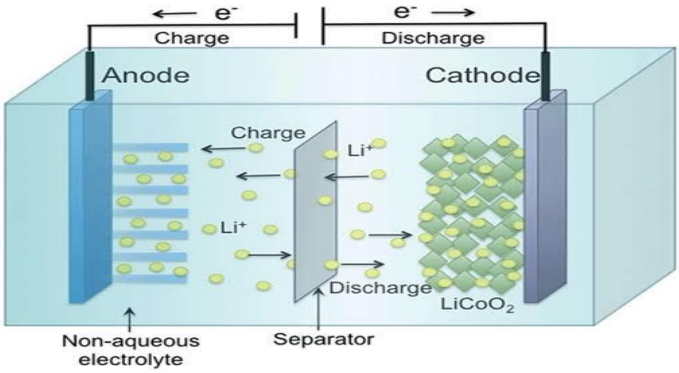

Fig 3.1: Working of Lithium-ion Battery

batteries present a high efficiency and a long-life span. Li-ion batteries are deployed in stationary energy storage applications and backup power applications. Another important advantage of this technology, in comparison to other battery technologies, is the high-capacity utilization even at high currents.

- Types Of Batteries

- Lead acid batteries Lead acid batteries are the common energy storage devices for PV systems. Lead acid batteries can be either 6V or 12V type in tough plastic container. The batteries can be flooded cell type or sealed/gel type.
- Flooded cell type battery This is the most commonly used type of battery for renewable energy systems today. Flat and Tubular plate type are the versions of flooded batteries. In flooded batteries the electrodes are completely submerged in the electrolyte. During charging of flooded batteries to full state of charge, hydrogen and oxygen gases produced from water by the chemical

reaction at negative and positive plates passes out through vents of the battery. This necessitates the periodic water addition to the battery.

- Sealed /Gel type battery These batteries have immobilized form of electrolyte. The sealed maintenance free lead acid batteries are also called as valve regulated lead acid (VRLA) batteries or captive electrolyte lead acid batteries. The sealed batteries are of two types namely gelled electrolyte type and absorbed glass mat type. Immobilized electrolyte batteries will have less electrolyte freeing problems compared to flooded electrolyte batteries. During charging process, hydrogen and oxygen gases are produced from water due to chemical reactions at the negative and positive plates. These gasses recombine to form water, thus the need for water additions is eliminated. This type of lead acid batteries is suitable for PV applications because of the following reasons: 1. Easy transportation. 2. Suitable for remote applications because of less maintenance requirement. 3. No need for water additions.
- Gelled batteries the addition of silicon dioxide to the electrolyte forms a warm liquid which is added to the battery and become gel after cooling. The hydrogen and oxygen produced during charging process are transported between positive and negative plates through the cracks and voids in the gelled electrolyte during the process of charge and discharge.
- Absorbed GAS MAT [AGM] batteries In AGM batteries the glass mats are sandwiched between plates. These glass plates absorb the electrolyte. The oxygen molecules from positive plate moves through the electrolyte in the glass mats and recombine hydrogen at the negative plate to form water. Both gel and AGM batteries require controlled charging. In these batteries generally Lead calcium electrode are used to minimize gassing and water loss. Voltage and current must be controlled below C/20 rate. Characteristics of Lead Acid Batteries: Specific energy: 25 – 35Wh/kg Life time: 250 -750 cycles Advantages: low cost, high efficiency, simple operation Disadvantages: relatively low lifetime

- Nickel –Cadmium (Ni - Cd) batteries In Ni-Cd battery positive electrode is made up of cadmium and the negative electrode by Nickel hydroxide separated by Nylon separators immersed in potassium hydroxide electrolyte placed in a stainless-steel casing. It has longer deep cycle life and temperature tolerant compared lead-acid battery. Cadmium is replaced by metal hydrides due to environmental regulatory rules. Memory effect degrades the battery capacity when the battery is idle for long time. Memory effect is the process of remembering the depth of discharge in the past. If the battery is discharged to 25% repeatedly, it will remember it, and if the discharge is greater than 25%, the cell voltage will drop as shown in figure 4. To recover the full capacity the battery, it should be reconditioned by fully discharging and then fully charging once in few months.
- Nickel – Metal hydride (Ni MH) batteries It is an extension of NiCd batteries with high energy density. The anode is made up of metal hydride instead of NiCd. It has less memory effect and delivers high peak power. It is expensive than NiCd batteries and overcharging damages the battery easily. Characteristics of Nickel-metal hydride Batteries: Specific energy: 65 – 75Wh/kg, Life time: 700 cycles

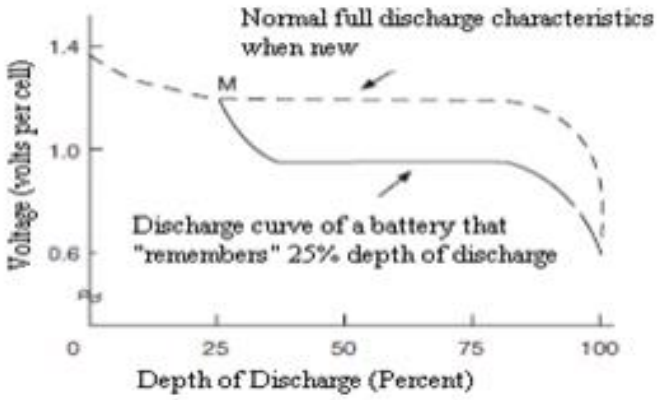

Fig 3.2. Memory effect of Ni-Cd battery

- Advantages: high specific energy, good deep discharge, environmental friendly Disadvantages: High cost, high self discharge and low efficiency 6.4 Lithium ion batteries The energy density of Li-ion batteries is 3 times that of Pbacid batteries. The cell voltage will be 3.5V, and few cells in series will give the required battery voltage. The lithium electrode reacts with the electrolyte creates a passivation film during every discharge and charge operation. This is compensated by the usage of thick electrodes. Because of this fact the cost of Li-ion battery is higher than NiCd batteries. Further overcharging damages the battery.
- Lithium polymer batteries in this battery solid polymer electrolyte acts as both electrolyte and separator and the lithium electrode reaction with the electrolyte is less.

➢ Battery Ageing Factors

Acid stratification: In lead acid batteries there is a slight difference in density between water and acid. If the battery is left idle for a long time, the mixture of water and acid can separate into layers with water rising up and acid sinking down because of gravimetric effects. This can lead to corrosion of the plates at the bottom side. The stratification can be removed by stirring the electrolyte with air pumps or nature gassing of the battery at high voltages.

Sulphation: Sulphation forms during normal operation of battery. During discharging process a thin layer of sulphate forms on the battery plates. The layer dissolves into the battery acid during charging. When a hard crystalline layer is formed it cannot dissolve during charging. When the sulphate crystals cover the surface area of the plates, it will reduce the battery efficiency by holding less charge. Sulphation occurs if the battery is kept idle for a long time or if the charging is not enough to dissolve the sulphate formed during charging cycle. Incomplete charging for long time and high temperature will also lead to sulphation. Desulphation can be carried out by equalization which is the process of overcharging the battery. Desulphation can also

be done by pulse conditioning by simply controlling the pulses or frequency components of frequency ranging 2-6 MHz.

Corrosion: The application high positive potential at the positive electrode causes the corrosion of the lead grid. It is an irreversible process and results in the decrease of cross section of grid which leads to the increase in grid resistance. Further formation of layers of lead oxide and sulphates between grid and active material increases the contact resistance which results in increased voltage drop during charging and discharging process. The factors on which corrosion depends are electrode potential, temperature, grid alloy and quality of grid. For PV applications batteries having thicker grid are suitable to minimise the corrosion effect and to increase the lifetime.

Erosion: The electrodes subjected to strong mechanical loads during cycling operation due to the conversion of active material into lead sulphate during discharge. Lead sulphate has 1.94 times larger than lead dioxide in volume per mole. Because of the change in volume, the active material loosens and gets separated from the electrode and forms sludge at the base of the battery. If the sludge volume becomes large then it may cause short circuit between electrodes. Short circuit. The plate connectors from the positive electrodes can also be subjected to corrosion and cause detachment of small layers of the connectors, which when fall on the electrodes will result in short circuit. To avoid these problem separators should extend upward over the electrodes. In case of lead acid batteries dendrites growing from positive to negative electrode through the separators. This growth can be accelerated by low state of charge for long periods which leads to low acid concentrations. This dendrite growth causes microscopic short circuit which will lead to sudden and complete breakdown of the battery.

Low temperature: Low temperature will not accelerate any irreversible aging effect. Formation of ice must be prevented. Once ice is formed, then it is difficult to operate the battery and the cell housing may burst due to the increased volume and the surroundings will be affected by the scattering of sulphuric acid.

High temperature: Increase of battery temperature by high ambient temperature or by

high current rate charging/discharging increase corrosion, sulphation, gassing and self discharge etc. For every 10°K rise of temperature the life time battery is reduced by 50%. The normal operating temperature for batteries is 10° - 20° C.

3.2 Designing of Battery

A. State of Charge Estimation:

The easiest way and most accurate method to measure the SoC is to use the direct relation of OCV (Open circuit voltage). This method can be used only when the battery has no current transfer. One needs to wait until all the cells of the battery reach steady state after charging or discharging is completed. Then the battery terminal voltage is directly measured. However, this method takes long time and can only be used for Offline SoC measurement. Presently the most common and practically used method for estimating SoC is coulometric method. Coulometric method integrates the charging or discharging current with respect to time to determine the estimated SoC. This method integrates current over time to get the amount of electric charge (C or Ah), which is then converted to the SoC. The SoC estimated by the coulometric method is given by

$SoC = (Qr \pm \int Idt) /(Qc)*100\%$

Where SoC is the present SoC, Qr is the amount of the charge present in the battery, I is the current that flows into or out of the battery, and Qc is the full capacity of the battery, which is equal to 4.95Ah. The recent capacity (Qr) can be obtained by the direct relation of OCV when the battery is at the steady state condition after being loaded. Qc is obtained by the datasheet of the battery.

B. Depth of Discharge:

Depth of discharge is defined as the total amount of energy that is discharged from a battery, divided by the battery nominal capacity. Depth of discharge is normally expressed as a percentage. For example, if a 100Ah battery is discharged for

20 minutes at a current of 50A, the depth of discharge is 50*20/60/100=16.7%

C. Battery Model:

The battery was modelled as a constant voltage source. However, as the battery charges and discharges, the value of its voltage also changes. This was not taken into account during the research as we only focus on the steady state of the converter. For that reason, the battery value will be changed manually during simulations. This is only considered when the battery is acting as a supplier of power. In order not to cause any trouble with the simulation, the same battery was modelled as a resistor with an appropriate value to draw the desired amount of power for the predetermined voltage. The equation used for this is the following:

$$|R| = \frac{V^2_{bat}}{P_{bat}} = \frac{nV_{DC-bus}V^3_{bat}}{2L*f_s} d(1-|d|) \text{……. (3.1)}$$

D. Battery Capacitor:

A capacitor was needed to provide a more steady voltage source in the battery. As it will be discussed later again in the DC-Bus capacitor, the main characteristic looked for was to have a voltage ripple specification lower than 5%.

For that reason, various calculations were taken into account, but more detail will be provided in the DC-Bus capacitor as, because of its changing nature, it makes more sense to explain it there. The calculations are totally transferable to this case just by changing the corresponding value of voltage, that is, substituting VDC−Bus by Vbat and obtaining:

$$C_{bat} = \frac{\Delta Q}{0.05*V_{bat}}. \quad \text{……. (3.2)}$$

The bidirectional converter local controller (LCBi) can operate in a neutral, voltage, or current control mode. For current control mode, two PI controllers were implemented to achieve a desired current reference, for the charging and discharging modes.

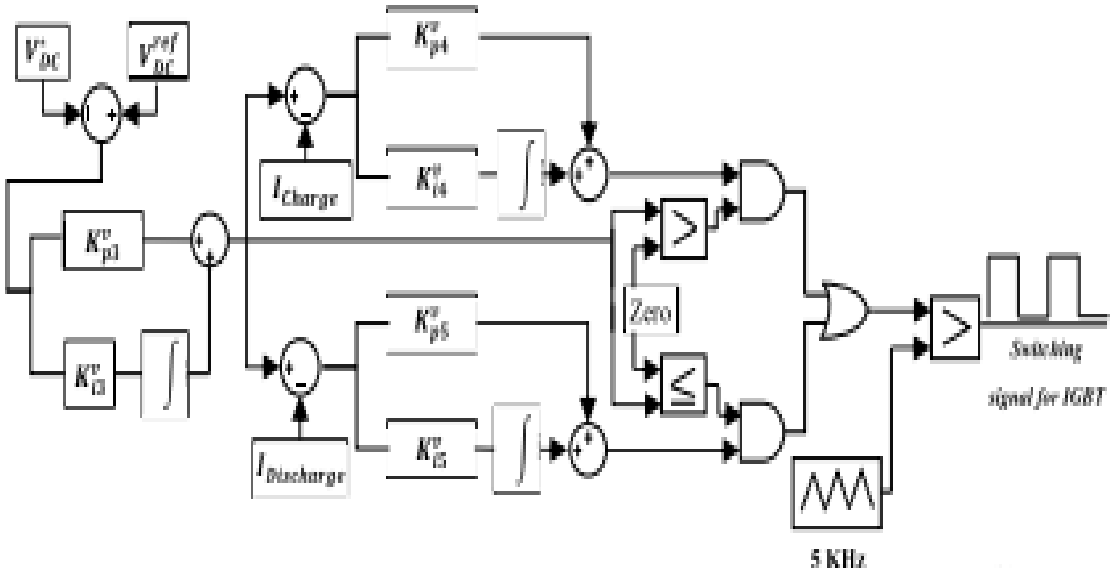

Fig 3.3: Bidirectional converter local controller

As for the voltage control, a nested PI was implemented. The values of Kp and Ki for both controllers are shown in the Appendix, Table A.VI. The transfer function for the LCBi, using the FSM could be derived as follows:

The transfer function for the charging current control is:

$$G_{ch}(S) = K_{p1}^{i}\left(I_{ch}^{ref} - I_{ch}^{*}\right) + \frac{K_{i1}^{i}}{s}\left(I_{ch}^{ref} - I_{ch}^{*}\right) \quad \text{……. (3.3)}$$

The transfer function for the discharging current control is:

$$G_{dch}(S) = K_{p2}^{i}\left(I_{dch}^{ref} - I_{dch}^{*}\right) + \frac{K_{i2}^{i}}{s}\left(I_{dch}^{ref} - I_{dch}^{*}\right) \quad \text{……. (3.4)}$$

The transfer function of the outer loop for voltage control is:

$$G_{v}^{bi}(S)\Big|_{ol} = K_{p3}^{v}\left(V_{DC}^{ref} - V_{DC}^{*}\right) + \frac{K_{i3}^{v}}{s}(V_{DC}^{ref} - V_{DC}^{*}) \quad \text{……. (3.5)}$$

In the nested PI controller, the outer loop yields the reference for the inner loop. Therefore, by substituting above, the nested PI controller transfer function, for maintaining the DC bus voltage will be:

$$G_v^{bi}(S) = \begin{cases} P_v^{bi}(m) * \left(\begin{matrix} K_{p4}^v \left(G_v(S) - I_{ch}^*\right) \\ + \dfrac{K_{i4}^v}{s} \left(G_v(S) - I_{ch}^*\right) \end{matrix} \right) V_{DC} > V_{ref} \\ P_v^{bi}(m) * \left(\begin{matrix} K_{p5}^v \left(G_v(S) - I_{dch}^*\right) \\ + \dfrac{K_{i5}^v}{s} \left(G_v(S) - I_{dch}^*\right) \end{matrix} \right) V_{DC} < V_{ref} \end{cases}$$

$$P_v^{bi}(m) = \sum_{j=0}^{2} \sum_{i=1}^{2} m_{i,j} = \begin{cases} 1 & (\exists m_{i,j} \in M)\, P_v^{bi}(m) = 1 \\ 0 & (\forall m_{i,j} \in M) P_v^{bi}(m) = 0 \end{cases}$$

the PI transfer function for charging/discharging the batteries through the bidirectional converter is:

$$G_i^{bi}(S) = \begin{cases} P_{i1}^{bi}(m) * \left(\begin{matrix} K_{p1}^i \left(I_{ref} - I_{ch}^*\right) \\ + \dfrac{K_{i1}^i}{s} \left(I_{ref} - I_{ch}^*\right) \end{matrix} \right) I_{ref} > 0 \\ P_{i2}^{bi}(m) * \left(\begin{matrix} K_{p2}^i \left(I_{ref} - I_{dch}^*\right) \\ + \dfrac{K_{i2}^i}{s} \left(I_{ref} - I_{dch}^*\right) \end{matrix} \right) I_{ref} \leq 0 \end{cases}$$

Where a single current reference is used. Depending on the sign of the reference current, the LCBi switches between charging and discharging modes

$$P_{i1}^{bi}(m) = m_{01} = \begin{cases} 1 & (\exists m_{i,j} \in M)\, P_{i1}^{bi}(m) = 1 \\ 0 & (\forall m_{i,j} \in M) P_{i1}^{bi}(m) = 0 \end{cases}$$

$$P_{i2}^{bi}(m) = \sum_{i=0}^{1} m_{0,2i} = \begin{cases} 1 & (\exists m_{i,j} \in M)\, P_{i2}^{bi}(m) = 1 \\ 0 & (\forall m_{i,j} \in M)\, P_{i2}^{bi}(m) = 0 \end{cases}$$

the state variables of the LCBi to maintain its various modes are the input/output currents and the output voltage of the bidirectional converter. Moreover, it can be seen that the set of event driven modes, {m20, m22, m10, m12, m21, m11, m01,m02} ⊆ M, commanded by the MGCC will have a direct impact on the operation of the LCBi.

CHAPTER 4

PROPOSED INVERTER WITH BLDC MOTOR

4.1 Introduction:

The DC-AC Converter, also known as the inverter, converts dc power to ac power at desired output voltage and frequency. The dc power input to the inverter is obtained from the dc bus. The filter capacitor across the input terminals of the inverter provides a constant dc link voltage. The inverter therefore is an adjustable-frequency voltage source.

Inverters can be broadly classified into two types, voltage source and current source inverters. A voltage–fed inverter (VFI) or more generally a voltage–source inverter (VSI) is one in which the dc source has small or negligible impedance. The voltage at the input terminals is constant. A current–source inverter (CSI) is fed with adjustable current from the dc source of high impedance that is from a constant dc source.

Voltage source inverter employing thyristors as switches, some type of forced commutation is required. While the VSIs made up of using GTOs, power transistors, power MOSFETs or IGBTs, self-commutation with base or gate drive signals for their controlled turn-on and turn-off. The dc to ac converters more commonly known as inverters, depending on the type of the supply source and the related topology of the power circuit, are classified as voltage source inverters (VSIs) and current source inverters (CSIs). Three-phase counterparts of the single-phase half and full bridge voltage source inverters are shown. Single-phase VSIs cover low-range power applications and three-phase VSIs cover medium to high power applications. The main purpose of these topologies is to provide a three-phase voltage source, where the amplitude, phase and frequency of the voltages can be controlled. The three-phase dc/ac voltage source inverters are extensively being used in motor drives, active filters and unified power flow controllers in power systems and uninterrupted power supplies to generate controllable frequency and ac voltage magnitudes using various

pulse width modulation (PWM) strategies. The standard three-phase inverter has six switches the switching of which depends on the modulation scheme. The input dc is usually obtained from a single-phase or three phase utility power supply through a diode-bridge rectifier and LC or C filter.

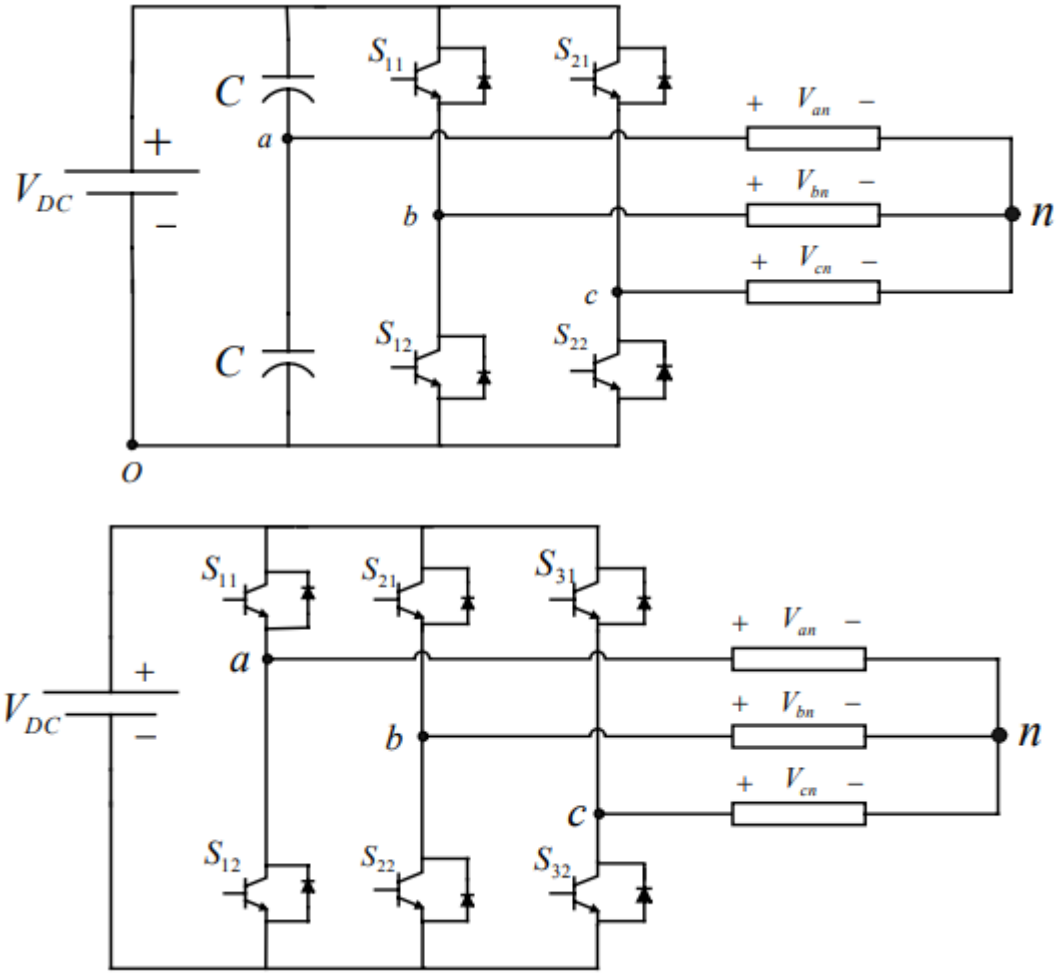

Fig 4.1: Structure of Inverter

The inverter has eight switch states given in Table. As explained earlier in order that the circuit satisfies the KVL and the KCL, both of the switches in the same leg cannot be turned ON at the same time, as it would short the input voltage violating the KVL.Thus the nature of the two switches in the same leg is complementary.

S11 + S12 =1

S21 + S22 =1

S31 + S32 =1

Table 4.1: The switching states in a three-phase inverter

S_{11}	S_{12}	S_{31}	V_{ab}	V_{bc}	V_{ca}
0	0	0	0	0	0
0	0	1	0	$-V_{DC}$	V_{DC}
0	1	0	$-V_{DC}$	V_{DC}	0
0	1	1	$-V_{DC}$	0	$-V_{DC}$
1	0	0	V_{DC}	0	$-V_{DC}$
1	0	1	V_{DC}	$-V_{DC}$	0
1	1	0	0	V_{DC}	$-V_{DC}$
1	1	1	0	0	0

Of the eight switching states as shown in Table, two of them produce zero ac line voltage at the output. In this case, the ac line currents freewheel through either the upper or lower components. The remaining states produce no zero ac output line voltages. In order to generate a given voltage waveform, the inverter switches from one state to another. Thus the resulting ac output line voltages consist of discrete values of voltages, which are -VDC, 0, and VDC. The selection of the states in order to generate the given waveform is done by the modulating technique that ensures the use of only the valid states.

$$\frac{V_{DC}}{2}(S_{11}-S_{12})=V_{an}+V_{no} \qquad \text{…….(4.1)}$$

$$\frac{V_{DC}}{2}(S_{21}-S_{22})=V_{bn}+V_{no}$$

$$\frac{V_{DC}}{2}(S_{31}-S_{32})=V_{cn}+V_{no}.$$

$$\frac{V_{DC}}{2}(M_{11})=V_{an}+V_{no}$$

$$\frac{V_{DC}}{2}(M_{21})=V_{bn}+V_{no}$$

$$\frac{V_{DC}}{2}(M_{31})=V_{cn}+V_{no}$$

$$\frac{V_{DC}}{2}(S_{11}+S_{21}+S_{31}-S_{12}-S_{22}-S_{32})=V_{an}+V_{bn}+V_{cn}+3V_{no}$$

$$\frac{V_{DC}}{6}(2S_{11}+2S_{21}+2S_{31}-3)=V_{no}$$

$$\frac{V_{DC}}{3}(2S_{11}-S_{21}-S_{31})=V_{an}$$

$$\frac{V_{DC}}{3}(2S_{21}-S_{21}-S_{31})=V_{bn}$$

$$\frac{V_{DC}}{3}(2S_{31}-S_{21}-S_{11})=V_{cn}.$$

…… (4.2)

4.2 Pulse Width Modulation Control:

There are three basic PWM techniques:

1. Single Pulse Width Modulation
2. Multiple Pulse Width Modulation
3. Sinusoidal Pulse Width Modulation

The fundamental magnitude of the output voltage from an inverter can be controlled to be constant by exercising control within the inverter itself that is no external

control circuitry is required. The most efficient method of doing this is by Pulse Width Modulation (PWM) control used within the inverter. In this scheme the inverter is fed by a fixed input voltage and a controlled ac voltage is obtained by adjusting the on and the off periods of the inverter components.

The advantages of the PWM control scheme are,

a) The output voltage control can be obtained without addition of any external components.

b) PWM minimizes the lower order harmonics, while the higher order harmonics can be eliminated using a filter.

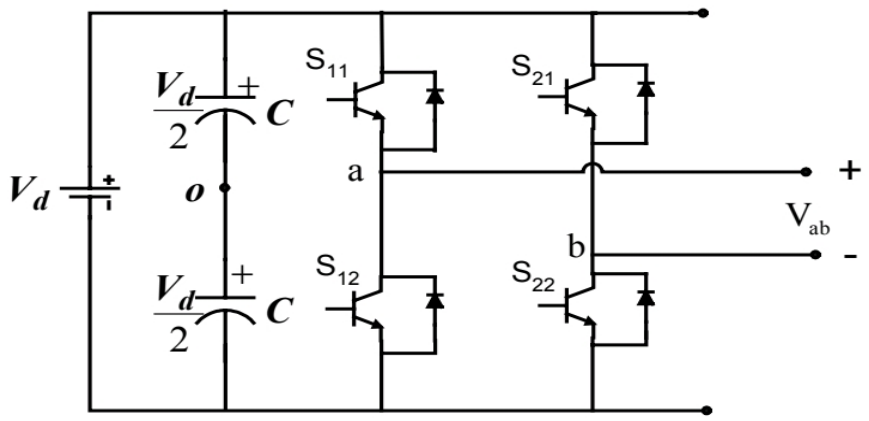

Fig 4.2: Single Phase Full-Bridge Inverter

The disadvantage possessed by this scheme is that the switching devices used in the inverter are expensive as they must possess low turn on and turn off times, nevertheless PWM operated are very popular in all industrial equipment's. PWM techniques are characterized by constant amplitude pulses with different duty cycles for each period. The width of these pulses are modulated to obtain inverter output voltage control and to reduce its harmonic content. There are different PWM techniques which essentially differ in the harmonic content of their respective output voltages, thus the choice of a particular PWM technique depends on the permissible harmonic content in the inverter output voltage.

Single-phase VSI Using PWM Modulation Technique:

A single-phase inverter in the full bridge topology is as shown in Fig 4.2, which consists of four switching devices, two of them on each leg. The full bridge inverter can produce an output power twice that of the half-bridge inverter with the same input voltage. The top devices are assigned to be S11 and S21 while the bottom deviceasS12andS22.The voltage equations for this converter are as given in the following equations.

$$\frac{V_d}{2}(S_{11} - S_{12}) = V_{an} + V_{no} = V_{ao} \ldots\ldots\ldots (4.3)$$

$$\frac{V_d}{2}(S_{21} - S_{22}) = V_{bn} + V_{no} = V_{bo} \ldots\ldots\ldots (4.4)$$

Table 4.2: Switching Pattern for the Bipolar Switching Scheme.

$$V_{ab} = V_{an} - V_{bn} \ldots\ldots\ldots (4.5)$$

$\mathbf{S_{11}}$	$\mathbf{S_{12}}$	$\mathbf{S_{21}}$	$\mathbf{S_{22}}$	$\mathbf{V_{An}}$	$\mathbf{V_{Bn}}$	$\mathbf{V_o(t) = V_{An}(t) - V_{Bn}(t)}$
ON	-	-	ON	V_d	0	V_d
-	ON	ON	-	0	V_d	-V_d
ON	-	ON	-	V_d	V_d	0
-	ON	-	ON	0	0	0

The voltages V_{an} and V_{bn} are the output voltages from phases A and B to an arbitrary point n,$V_{an}$is the neutral voltage between point n and the mid-point of the DC source. The switching function of the devices can be approximated by the Fourier series to be equal to $\frac{1}{2}(1 + M)$ where M is the modulation signal which when compared with the triangular waveform yields the switching pulses.

Thus, from Equations the expressions for the modulation signals are obtained as

$$M_{11} = \frac{2(V_{an}+V_{no})}{V_d} \ldots\ldots\ldots (4.6)$$

$$M_{21} = \frac{2(V_{bn}+V_{no})}{V_d} \ldots\ldots\ldots (4.7)$$

SPWM With Bipolar Switching Scheme:

The switching pattern along with the sine-triangle comparison is as shown in Figure. The switching pattern for positive values of modulating signal V is as given

$V_r > V_c$, S_{21} is on

$V_r < V_c$, S_{21} is on

The switching pattern for negative values of the modulating signal V is given as

$V_r < V_c$, S_{21} is on

$V_r > V_c$, S_{22} is on

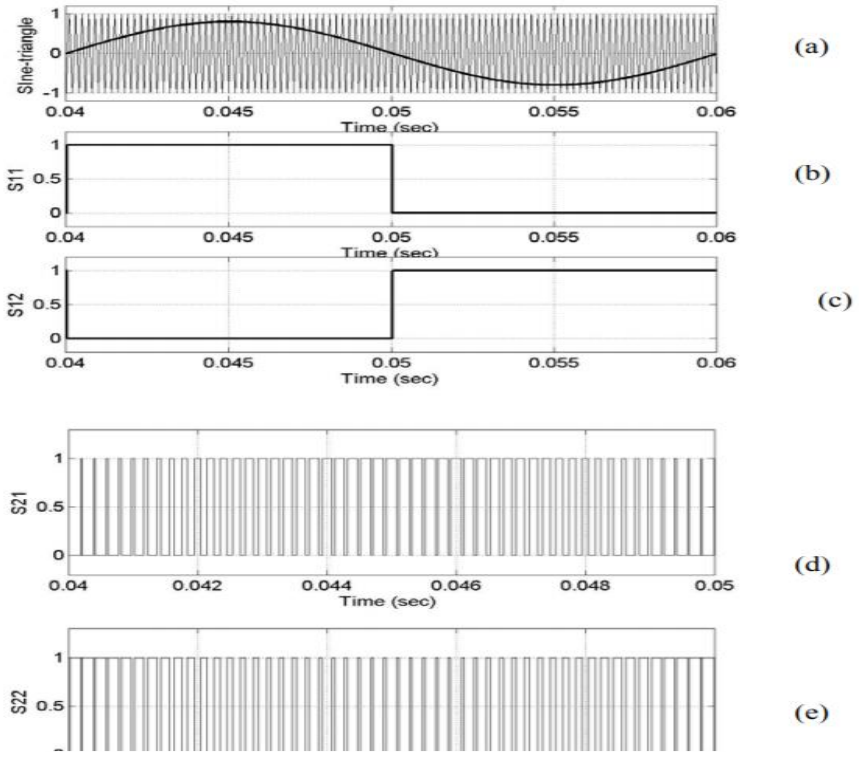

Fig 4.3: Bipolar PWM Scheme (a) Sine -Triangle Comparison (b), (c), (d) & (e)

The output voltage is given as $V_o(t) = V_{An}(t) - V_{Bn}(t)$, as shown in Fig 2.15. The load current is also shown in the same plot. The switching pattern for the Bipolar Switching Scheme is as given in Table.

Fig 4.4: Bipolar PWM Scheme (a) Line to Line Voltage (b) Load Current

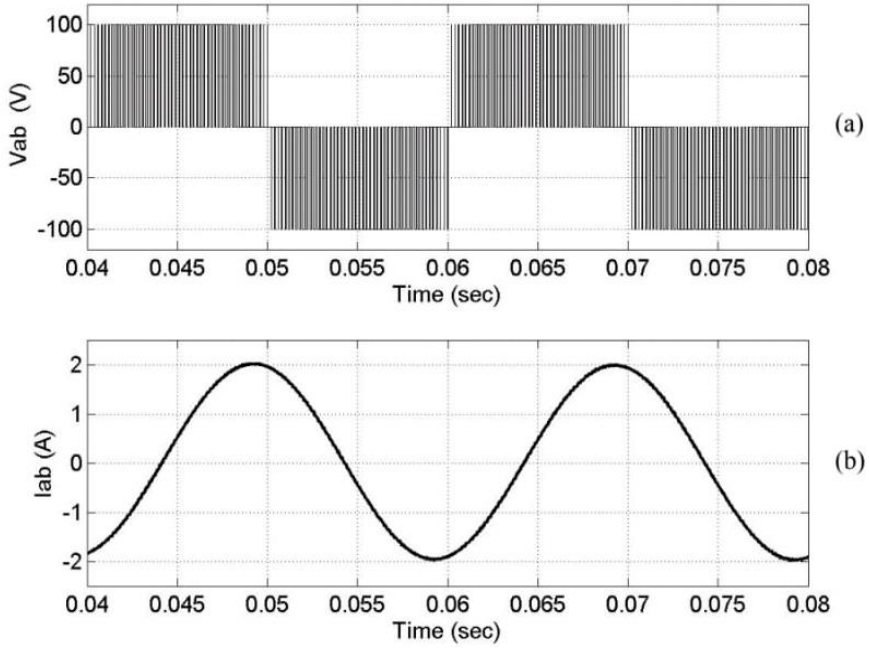

From Table -it can be observed that when the two top or the two bottom devices are turned on the output voltage is zero. In the bipolar switching scheme, the output voltage level changes between either 0 to -V_d or from 0 to +V_d . Since the sign of the modulation signal decides the switching pattern the analysis of this switching scheme is complex. The relationship between input and output voltage is given as

$V_o = mV_d$ Where m=0.5($m_i + \frac{4}{\pi}$) ($m_i < 1.0$)

4.3BLDC motor

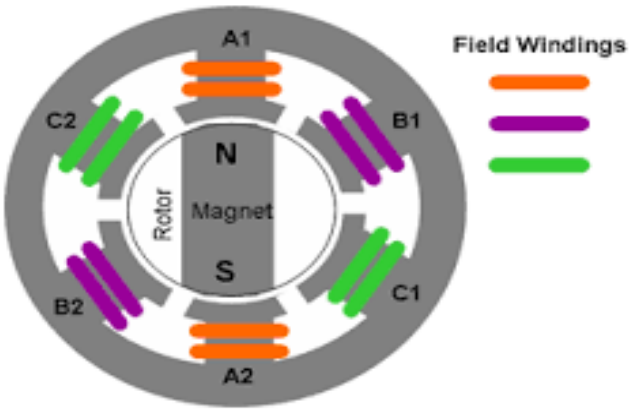

Fig 4.5: The internal structure of BLDC motor

The high gain boosted output will be fed to the three-phase inverter which converts into three phase AC output and is fed to the BLDC motor. BLDC motor drives, systems in which a permanent magnet excited synchronous motor is fed with a variable frequency inverter controlled by a shaft position sensor. There appears a lack of commercial simulation packages for the design of controller for such BLDC motor drives. One main reason has been that the high software development cost incurred is not justified for their typical low cost fractional/integral kW application areas such as NC machine tools and robot drives, even it could imply the possibility of demagnetizing the rotor magnets during commissioning or tuning stages. Nevertheless, recursive prototyping of both the motor and inverter may be involved in novel drive configurations for advance and specialized applications, resulting in high developmental cost of the drive system. Improved magnet material with high (B.H), product also helps push the BLDC motors market to tens of kW application areas where commissioning errors become prohibitively costly. Modelling is therefore essential and may offer potential cost savings. A brushless dc motor is a dc motor turned inside out, so that the field is on the rotor and the armature is on the stator. The brushless dc motor is actually a permanent magnet ac motor whose torque-current characteristics mimic the dc motor. Instead of commutating the

armature current using brushes, electronic commutation is used. This eliminates the problems associated with the brush and the commutator arrangement, for example, sparking and wearing out of the commutator-brush arrangement, thereby, making a BLDC more rugged as compared to a dc motor. Having the armature on the stator makes it easy to conduct heat away from the windings, and if desired, having cooling arrangement for the armature windings is much easier as compared to a dc motor. In effect, a BLDC is a modified PMSM motor with the modification being that the back-emf is trapezoidal instead of being sinusoidal as in the case of PMSM. The "commutation region" of the back-emf of a BLDC motor should be as small as possible, while at the same time it should not be so narrow as to make it difficult to commutate a phase of that motor when driven by a Current Source Inverter. The flat constant portion of the back emf should be 120° for a smooth torque production. The position of the rotor can be sensed by using an optical position sensor and its associated logic. Optical position sensors consist of phototransistors (sensitive to light), revolving shutters, and a light source. The output of an optical position sensor is usually a Logical signal.

A brush less dc motor is defined as a permanent synchronous machine with rotor position feedback. The brushless motors are generally controlled using a three phase power semiconductor bridge. The motor requires a rotor position sensor for starting and for providing proper commutation sequence to turn on the power devices in the inverter bridge. Based on the rotor position, the power devices are commutated sequentially every 60 degrees. Instead of commutating the armature current using brushes, electronic commutation is used for this reason it is an electronic motor. This eliminates the problems associated with the brush and the commutator arrangement, for example, sparking and wearing out of the commutator brush arrangement, thereby, making a BLDC more rugged as compared to a dc motor. The brush less dc motor consist of four main parts power converter, permanent magnet-synchronous machine (PMSM) sensors, and control algorithm. The power converter transforms power from the source to the PMSM which in turn converts electrical energy to

mechanical energy. One of the salient features of the brush less dc motor is the rotor position sensors, based on the rotor position and command signals which may be a torque command ,voltage command ,speed command and so on the control algorithms determine the gate signal to each semiconductor in the power electronic converter. The structure of the control algorithms determines the type of the brush less dc motor of which there are two main classes voltage source-based drives and current source-based drives. Both voltage source and current source-based drive used with permanent magnet synchronous machine with either sinusoidal or non-sinusoidal back emf waveforms. Machine with sinusoidal back emf may be controlled so as to achieve nearly constant torque. However, machine with a non-sinusoidal back emf offer reduces inverter sizes and reduces losses for the same power level.

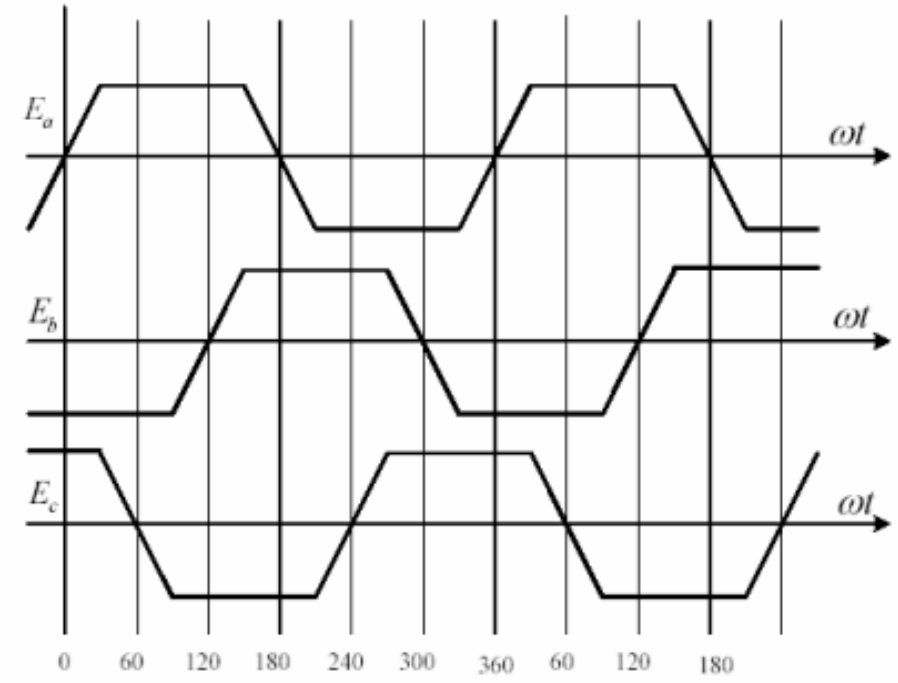

Fig 4.6: Trapezoidal back emf of three phase BLDC motor

The hall signals generated from the BLDC motor are converted into switching pulses to the inverter. BLDC motor has been chosen due to its advantages like higher

efficiency, higher reliability, capable of providing large amount of power over wide range of speeds. The construction of BLDC motor can be explained with two main parts namely stator and rotor. The stator consists of steel laminations with slots provided for the windings to be placed which can be arranged in either star or delta connection. The rotor is made up of two permanent magnets where the poles may vary based up on the application. The other part of the BLDC motor is hall sensor which works on the principle of Hall Effect that is when the current carrying conductor is placed in a magnetic field, charge carriers experience forces whose magnitude is based up on the voltage generated. If the direction of magnetic field is reversed, the voltage generated also reverses. Whenever the two magnetic poles pass near the hall sensor, the hall sensor generate signal which determines the position of the shaft and whose number is three which produces the exact sequence of commutation.

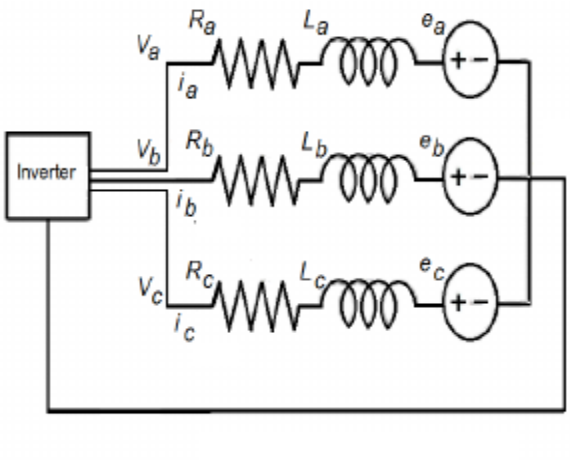

Fig 4.7: Dynamic Model of BLDC Motor

The above figure shows the dynamic model of BLDC motor which consists of winding resistances and inductances and generated EMF'S. The equations for the voltages across the armature windings can be given as

$$V_a = i_a R_a + L_a \frac{di_a}{dt} + e_a \text{……. (4.8)}$$

$$V_b = i_b R_b + L_b \frac{di_b}{dt} + e_b \quad \text{……. (4.9)}$$

$$V_c = i_c R_c + L_c \frac{di_c}{dt} + e_c \qquad \text{……. (4.10)}$$

The expression for the back emf in terms of rotor angle can be given as

$$e_a = \theta_e w \qquad \text{……. (4.11)}$$

$$e_b = (\theta_e - 120)w \qquad \text{……. (4.12)}$$

$$e_c = (\theta_e - 240)w \qquad \text{……. (4.13)}$$

The electromagnetic torque can be expressed as

$$T_e = \frac{(e_a i_a + e_b i_b + e_c i_c)}{w} \qquad \text{……. (4.14)}$$

The mechanical torque transferred to shaft can be given as

$$T_e - T_l = J \frac{dw}{dt} + Bw \qquad \text{……. (4.15)}$$

CHAPTER 5

SIMULATION AND RESULTS

5.1 Specification of the Proposed System

Below is the Simulation specification table for the proposed system. In order to verify the performance of the proposed system, at first, simulations have been done in ideal, battery discharging and charging modes by MATLAB software.

Table 5.1: Simulation Specifications of the proposed system

Sl. No	Objects	Values
1	Maximum PV module Voltage	51.6 V
2	Maximum PV module Current	9.7 A
3	Maximum PV module Power	500.5 W
4	BLDC Voltage	220 V
5	ITPC input voltage	51.6 V
6	ITPC output voltage	220 V
7	ITPC input current	9.7 A
8	ITPC output current	2.2 A
9	Converter switching frequency	24 KHZ
10	Converter Duty Cycle	81%
11	BLDC torque	4 N-m
12	BLDC speed	1250 RPM

5.2 Simulation Diagram and Results of Proposed System

The proposed system has been simulated using MATLAB and below figures shows the simulation diagrams in proposed system.

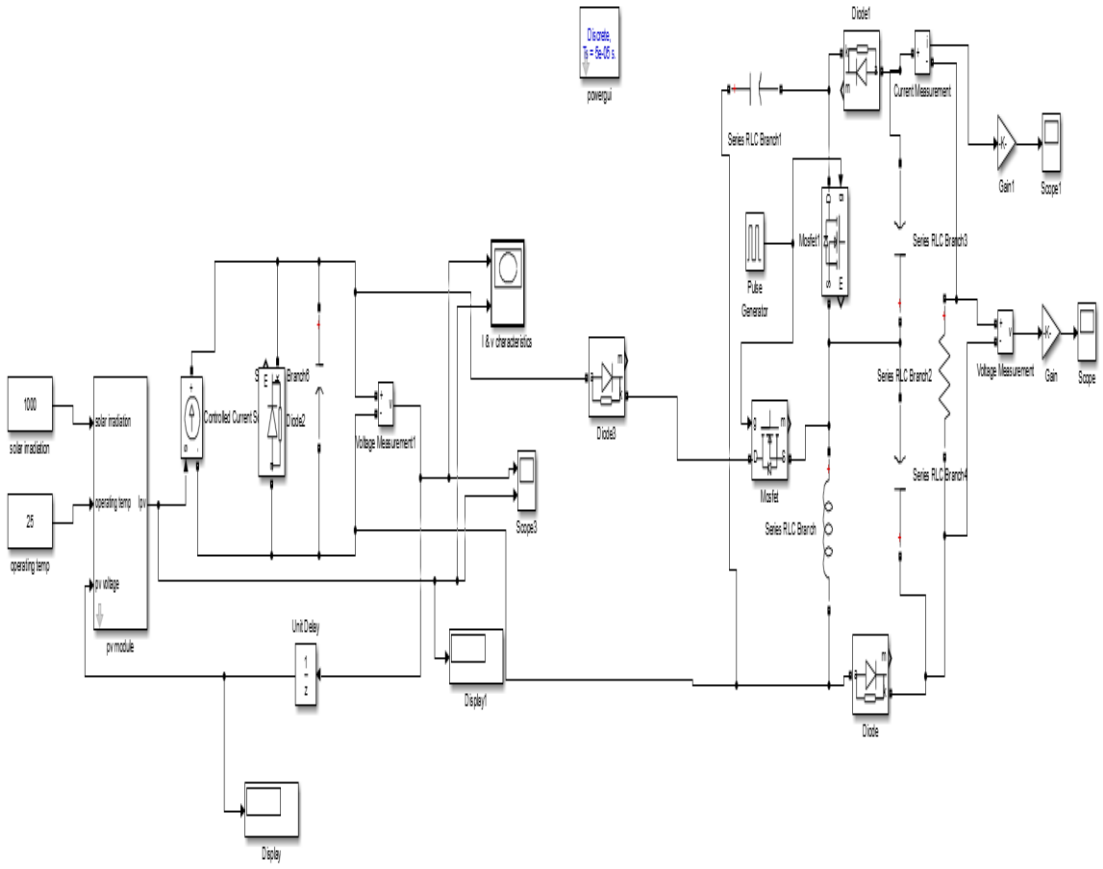

Fig 5.1: Simulation diagram of proposed system in PV mode

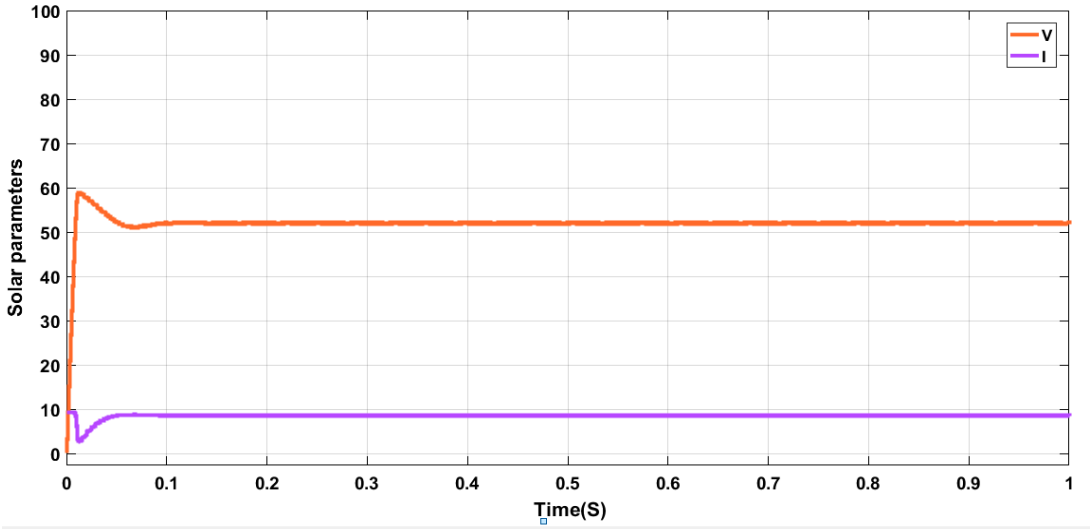

Fig 5.2: Proposed system parameters

The above waveform represents parameters of solar panel whose voltage is expressed in volts and current in Amps and its output is fed to converter.

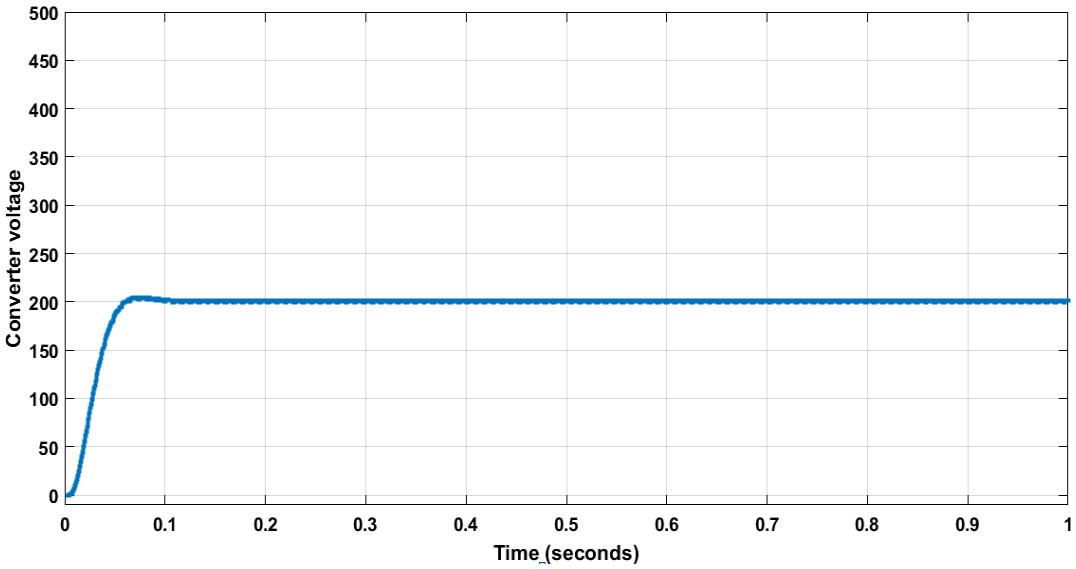

Fig5.3: Converter Voltage

The above waveform represents converter voltage plotted between voltage on Y-axis and time on X-axis. Voltage is expressed in volts whereas time is expressed in Seconds.

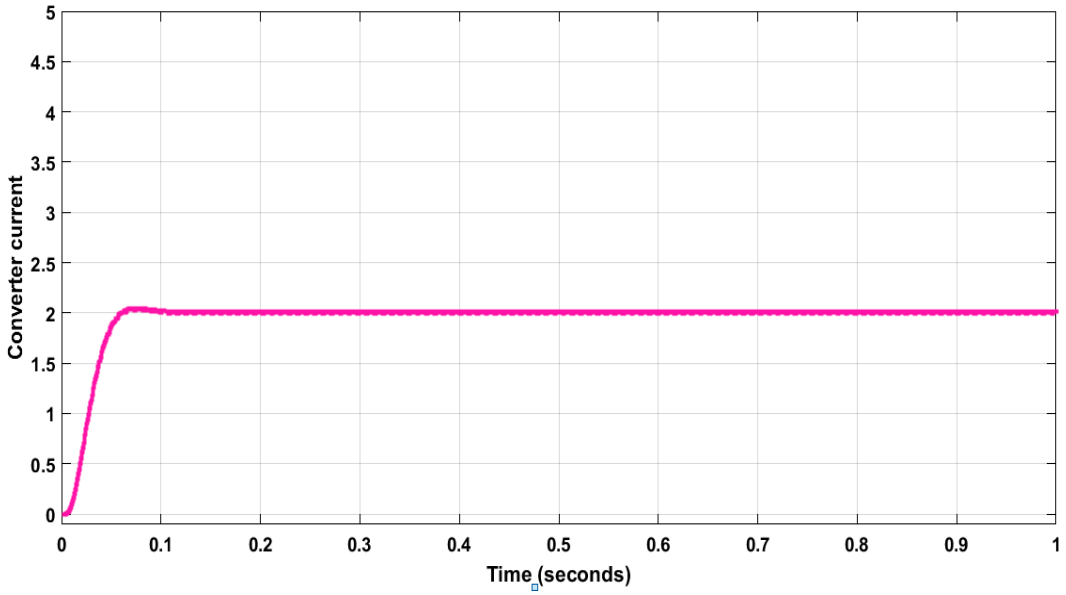

Fig5.4: Converter Current

The above Waveform represents converter characteristics where current is taken on Y-axis in Amps and time is taken on X-axis in Seconds.

5.3 PID Controller with MPPT technique

The below simulation diagram shows the proposed system when connected to PID with MPPT controller.

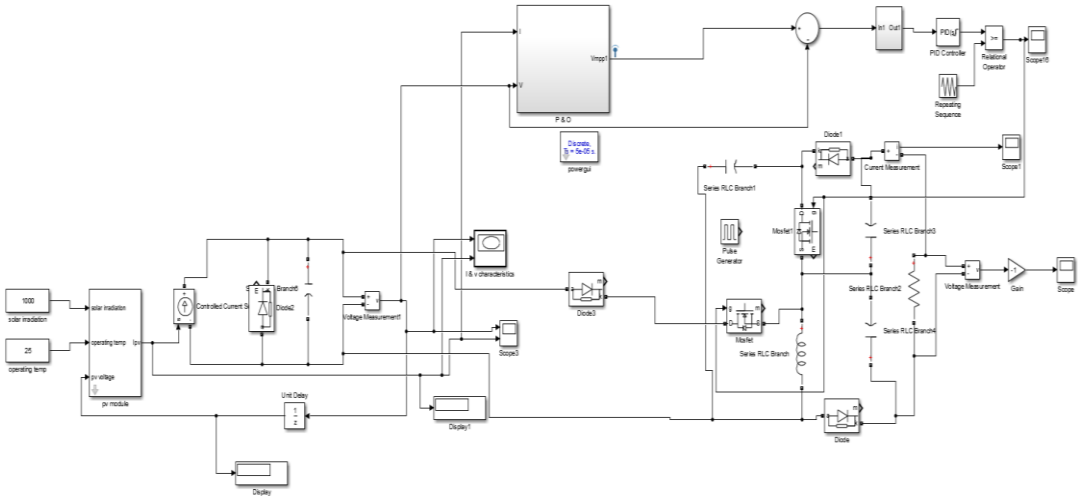

Fig 5.5Simulation diagram of Proposed system connected to PID with MPPT

The below are the waveforms of Proposed system when connected to PID with MPPT controller.

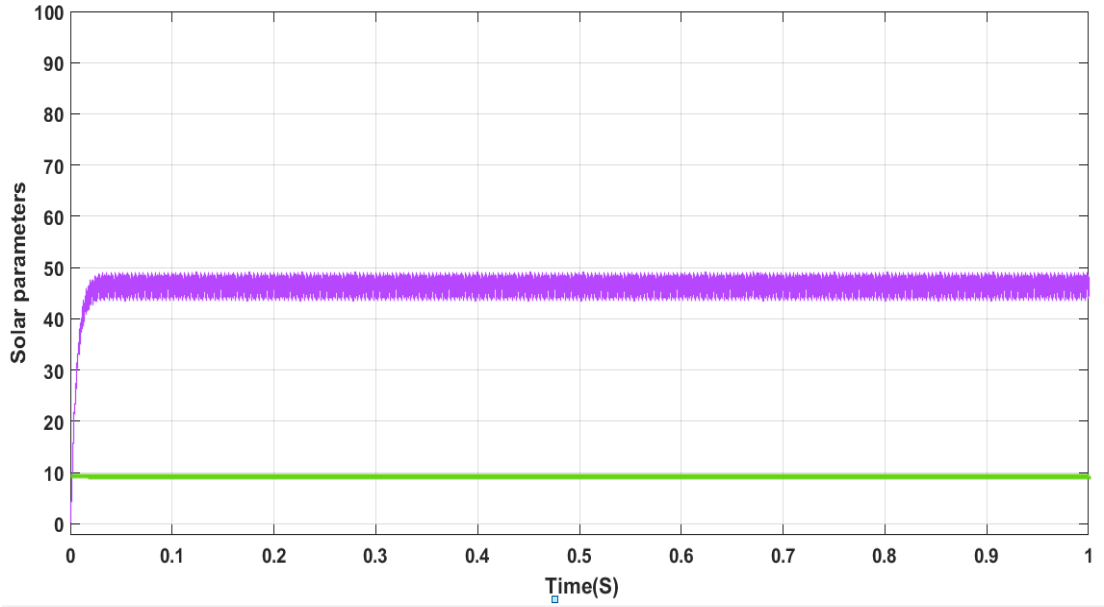

Fig 5.6(a): Solar Parameters of PID controller with MPPT Technique

The above waveform represents solar parameters when PID controller with MPPT technique is used. Here voltage in volts is taken on Y-axis and time in seconds is plotted on X-axis.

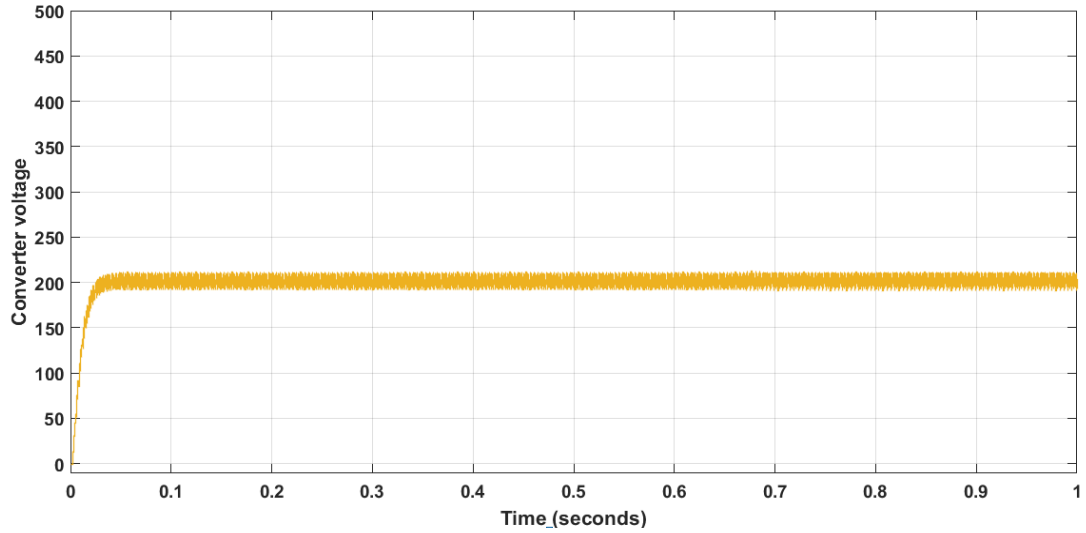

Fig 5.6(b): Converter voltage of PID controller with MPPT Technique

The above waveform in fig 5.5(b) represents converter voltage when PID controller with MPPT technique is used. Here voltage in volts is taken on Y-axis and time in seconds is plotted on X-axis.

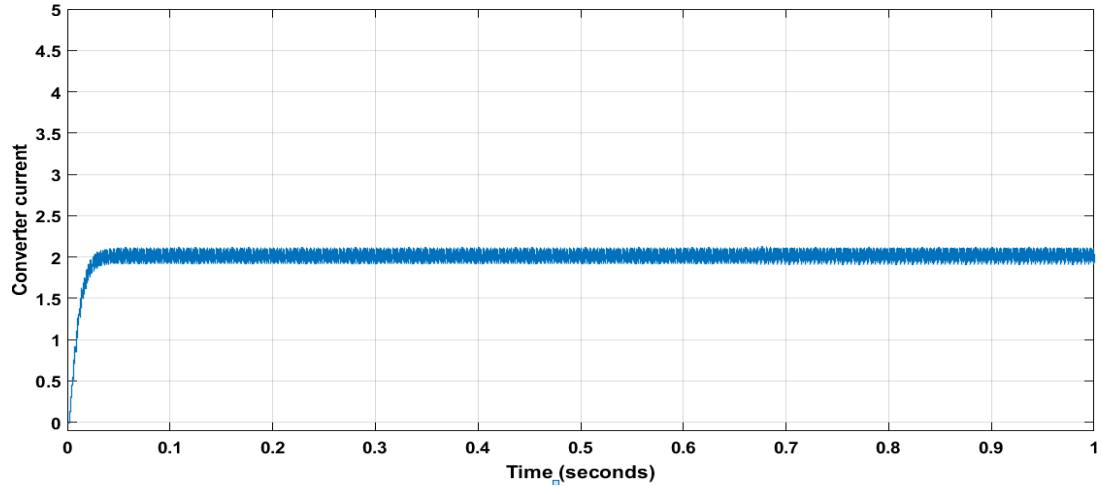

Fig 5.6(c): Converter Current of PID controller with MPPT Technique

Fig 5.6(a), (b), (c): PID controller with MPPT technique

The above waveform in fig 5.5(c) represents converter current when PID controller with MPPT technique is used. Here current in Amps is taken on Y-axis and time in seconds is plotted on X-axis.

5.4 Fuzzy controller with MPPT Technique

Below is the simulation diagram which represents the proposed system when connected to Fuzzy controller with MPPT technique.

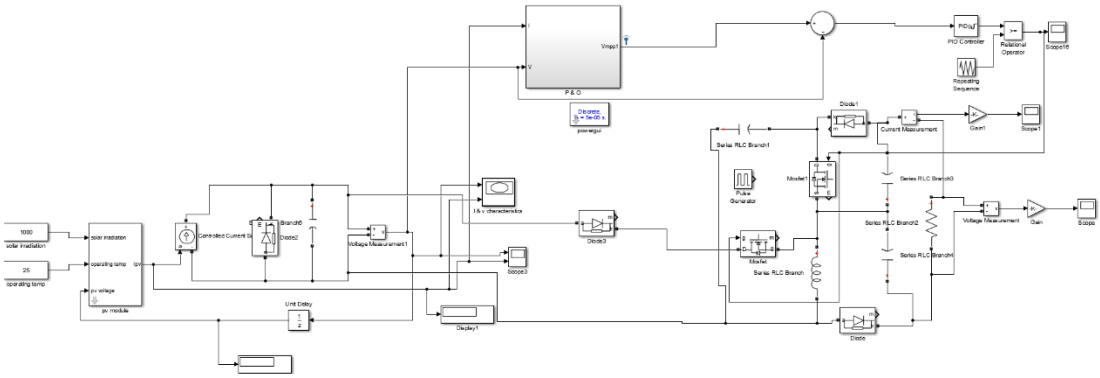

Fig 5.7: Simulation diagram of proposed system with fuzzy controller

Below are the waveforms associated to proposed system when connected to fuzzy controller with MPPT technique.

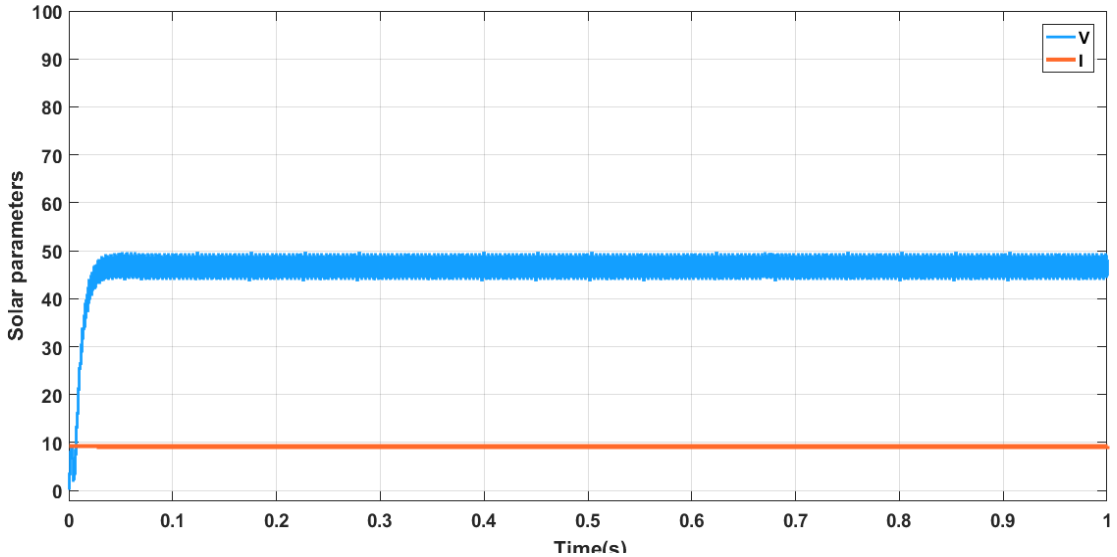

Fig 5.8(a): Solar Parameters of Fuzzy controller with MPPT Technique

The above figure represents Proposed system's solar parameters when connected to fuzzy controller with MPPT technique. The blue line indicates Voltage in volts on Y-axis Vs Time in seconds taken on X-axis and Red line indicates Current in Amps on Y-axis Vs Time in seconds taken on X-axis.

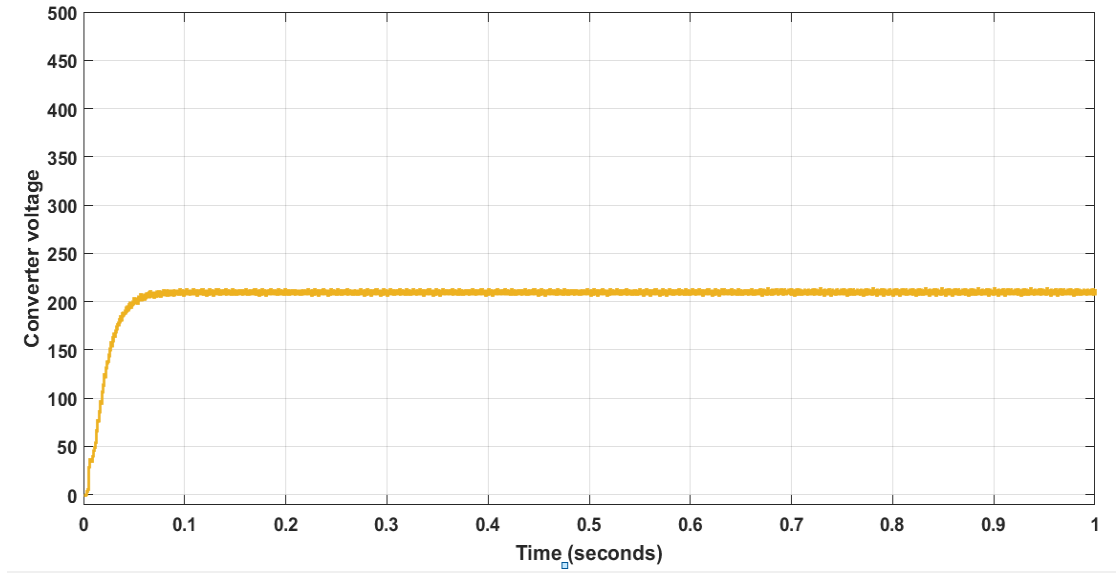

Fig 5.8(b): Converter Voltage of Fuzzy controller with MPPT Technique

The above fig 5.7(b) represents converter voltage when fuzzy controller with MPPT technique is used. Voltage in volts is taken on Y-axis and Time in seconds is taken on X-axis.

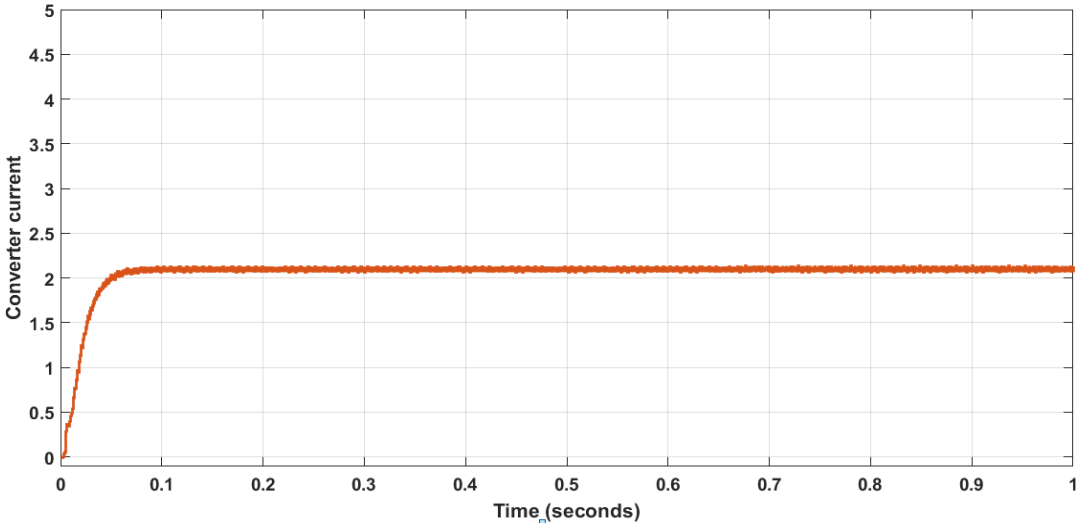

Fig 5.8(C): Converter Current of Fuzzy controller
Fig5.8(a), (b), (c): Fuzzy Controller with MPPT Technique

The above fig 5.8(c) represents converter current when fuzzy controller with MPPT technique is used. Current in Amps is taken on Y-axis and Time in seconds is taken on X-axis.

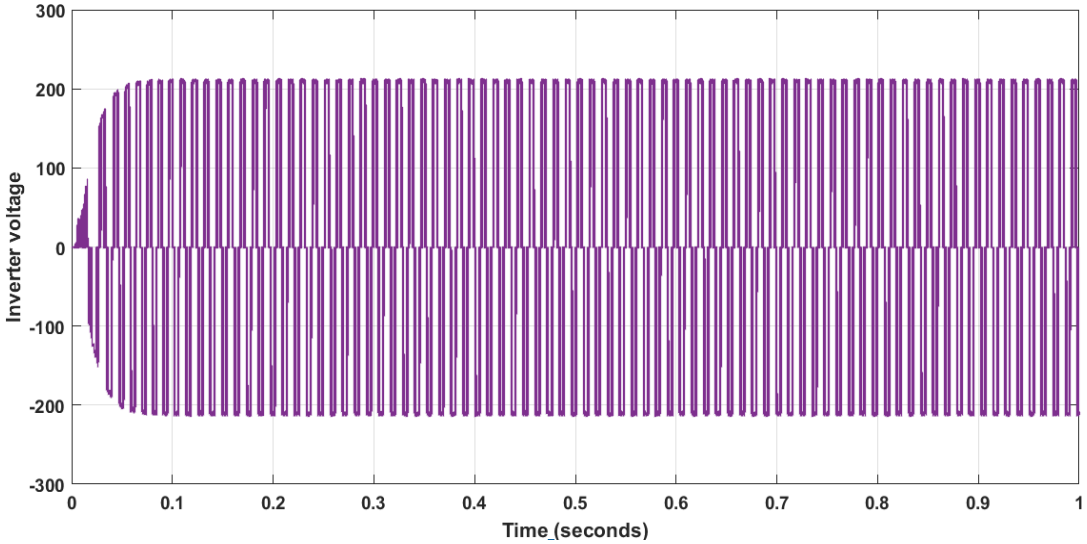

Fig 5.9: Inverter voltage

The above waveform represents inverter characteristics where inverter voltage in volts is plotted on Y-axis and time in seconds is taken on X-axis.

5.5 Battery Parameters

The output of converter is fed to battery for backup purpose whose parameters are shown in below waveform. The battery parameters are plotted for both battery charging domain and battery discharging domain. Also the ideal conditions are also considered.

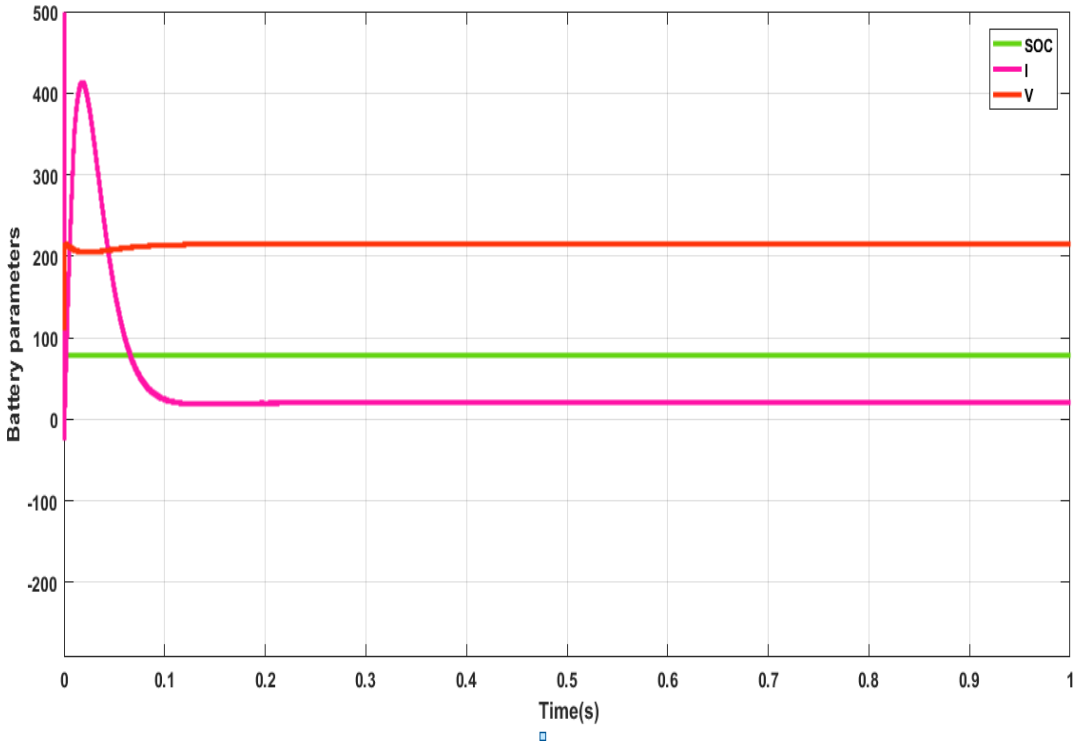

Fig 5.10: Battery Parameters

The SOC(State of Charge) is represented in green line which reads 80%.The curve doesn't deviate more in three different domains (charging, discharging, ideal). And the pink line indicates current in Amps waveform under battery domain. The red line indicates Voltage in volts which reads 200V.

5.6 BLDC Parameters

The below simulation diagram shows the proposed system when connected to BLDC motor. The input to BLDC is fed from inverter.

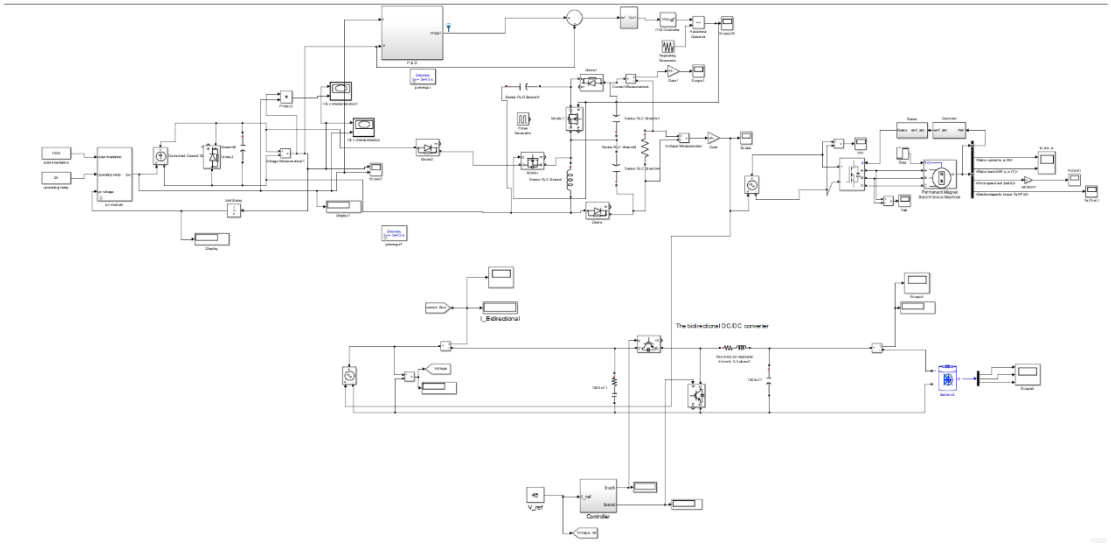

Fig 5.11: Simulation diagram of proposed system when connected to BLDC motor

The below waveforms represent output of BLDC motor when it is connected to inverter at input side.

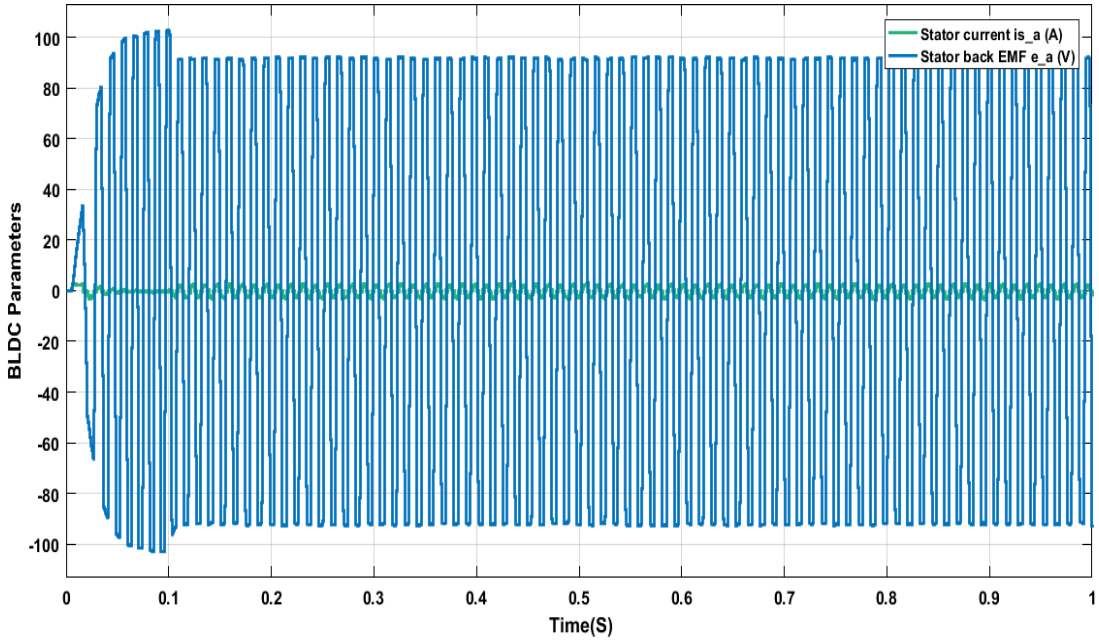

Fig 5.12(a): BLDC Parameters

The above waveform represents how stator current in Amps and stator back emf in volts varies with time taken on X-axis in seconds.

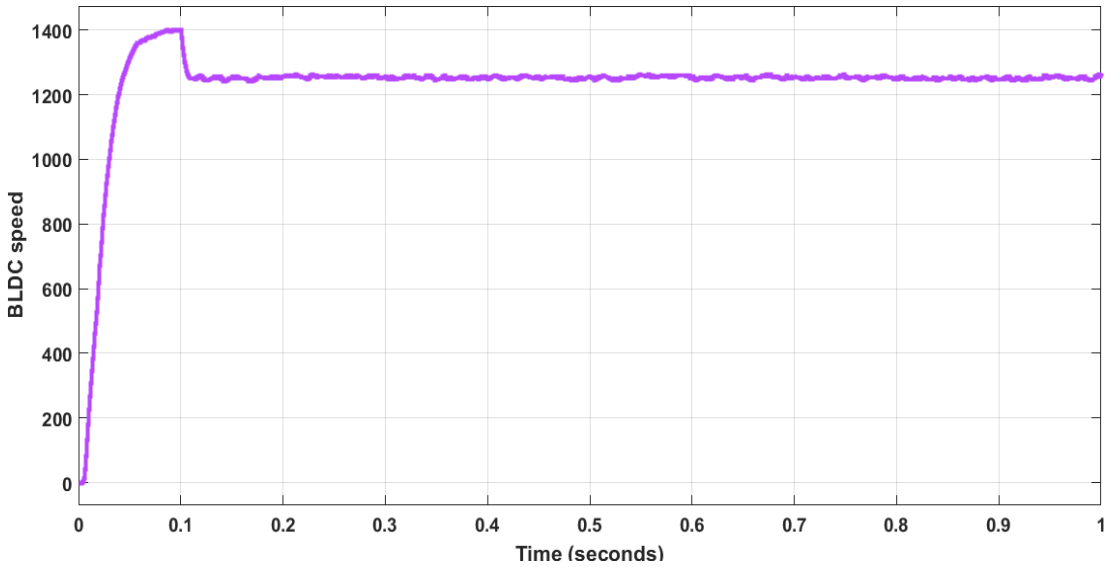

Fig 5.12(b): BLDC speed

The above waveform represents how the BLDC motor speed in rpm varies with time in seconds. Speed of motor is taken on Y-axis and time is taken on X-axis.

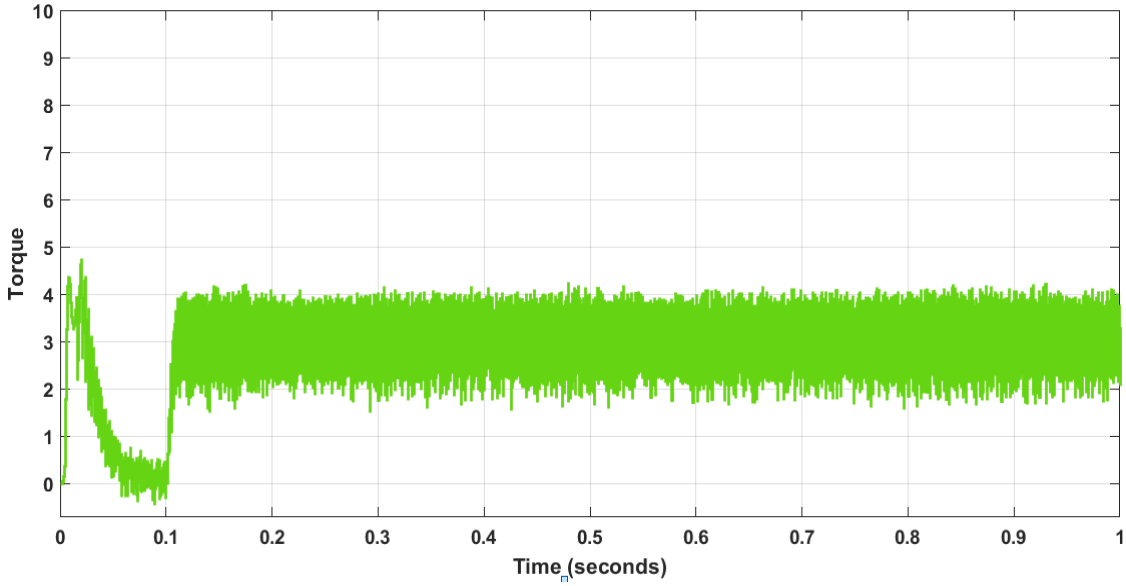

Fig 5.12(c): BLDC Torque

Fig5.12(a),5.12(b),5.12(c): BLDC Parameters

Torque Vs Time characteristics of BLDC motor are plotted in above figure.

Table 5.2: Comparison of results using various conductors

Parameter	**With MPPT**	**With PID MPPT**	**With Fuzzy MPPT**
Voltage	214	220	223
Current	1.9	2	2.1
Power	406.6	440	468.3
Settling time	0.1	0.07	0.05
Ripple %	14.2%	18.18%	4%

From the above table, it is clear that the ripple content is less in Fuzzy controller with MPPT technique for the proposed system. The percentage of ripple content reads around 4% only. Whereas the other techniques have more ripple contents: proposed system with PID controller has 18% and system with MPPT alone has 14% of ripple content in the output converter waveforms.

CHAPTER 6

CONCLUSION AND FUTURE SCOPE

6.1 Conclusion

The design of improved three interface converter, and B4-Inverter fed brushless direct electric current motor drive for industrial uses has been implemented in this project. The ITPC has been operated in unidirectional and going in both directions for accomplishing a built-in dual electric potential and power rate of flow control. It also involves design of MPPT controller to extract maximum power from the converter under various operating conditions. The static and dynamic response of the converter has been controlled with various controllers like PID controller and fuzzy controller and the comparison has been provided among various controllers. The results are validated by performing simulations of the proposed systems in MATLAB/Simulink.

The Three Port Converter (TPC) and B4-Inverter fed BLDC motor drive has been proposed targeting low or medium power applications. The TPC has been operated in unidirectional and bidirectional ways simultaneously for achieving an inherent dual voltage and power flow control. Furthermore, losses and efficiency of the proposed system are analyzed with three different domains, i.e., with battery charging, discharging, and PV systems effectively. The results have been validated by performing simulations of the proposed systems in MATLAB/Simulink. A detailed comparison has been made between the proposed converter and the predecessors to examine the benefits of the proposed converter. Experimentation has been performed using prototype models, the hardware results of which have closely resembled the simulation results. Moreover, a satisfactory closed-loop performance has been achieved for both simulation and experimental setup. Losses and efficiency of the proposed ITPC based system are compared with the existing TPC based system. The validation results reveal that the proposed converter has performed effectively under all the three domains and that the losses in the PV domain has been reduced

compared to the other converters. In addition, the average efficiency achieved has been 80.95%.

6.2 Future Scope

The outcomes of the experiment have validated the proposed model for different applications related to renewable sources and energy storage systems. Future work of the research will focus on the application of the proposed converter in the domain of agriculture, integrating renewables and energy storages.

REFERENCES

1. S. K. Shanmugam, S. Ramachandran, S. Arumugam, S. Pandiyan, A. Nayyar and E. Hossain, "Design and Implementation of Improved Three Port Converter and B4-Inverter Fed Brushless Direct Current Motor Drive System for Industrial Applications," in IEEE Access, vol. 8, pp. 149093-149112, 2020, doi: 10.1109/ACCESS.2020.3016011.
2. Shanmugam Sathish Kumar, Arumugam Senthil kumar, Palanirajan Gowtham, Ramachandran Meena kumari, Kanagaraj Krishna Kumar Implementation of solar photovoltaic array and battery powered enhanced DC-DC converter using B4-inverter fed brushless DC motor drive system for agricultural water pumping applications. Journal of Vibro engineering, Vol. 20, Issue 2, 2018, p. 1214-1233. https://doi.org/10.21595/jve.2018.19449
3. Deng, Junyun et al. “An Integrated Three-Port DC/DC Converter for High-Voltage Bus Based Photovoltaic Systems.” 2018 IEEE Energy Conversion Congress and Exposition (ECCE) (2018): 5948-5953.
4. S. Shuvo, E. Hossain, T. Islam, A. Akib, S. Padmanaban and M. Z. R. Khan, "Design and Hardware Implementation Considerations of Modified Multilevel Cascaded H-Bridge Inverter for Photovoltaic System," in IEEE Access, vol. 7, pp. 16504-16524, 2019.
5. B. Singh, S. Singh, A. Chandra, and K. Al-Haddad, “Comprehensive study of single-phase ac-dc power factor corrected converters with high frequency isolation,” IEEE Trans. Ind. In format., vol. 7, no. 4, pp. 540–556, Nov. 2011.
6. Sathish Kumar Shanmugam, Arumugam Senthil kumar, “Design and implementation of DC source fed improved dual-output buck-boost converter for agricultural and industrial applications. Journal of Vibro motoring, Vol. 19, Issue 8, 2017, p. 6433-6454.

7. Sathish Kumar Shanmugam, Arumugam Senthil kumar, "Implementation of solar photovoltaic array and battery powered enhanced DC-DC converter using B4-inverter fed brushless DC motor drive system for agricultural water pumping applications. Journal of Vibro motoring, Vol. 20, Issue 2, 2018, p. 1214-1233.
8. Frederick D. Kieferndorf, Member, IEEE, Matthia Forsterand ThomasA.Lipo, Fellow, IEEE,March/April- 2004. "Reduction of DC – Bus Capacitor Ripple Current with PAM/PWM Converter" IEEE Transactions on IndustryApplications, Vol. 40.No.2, pp.607-615.